Hf-Nd isotope and trace element constraints on subduction inputs at island arcs: limitations of Hf anomalies as sediment input indicators

Heather K. Handley[1,2*], Simon Turner[2], Colin G. Macpherson[1], Ralf Gertisser[3], Jon P. Davidson[1]

[1] Department of Earth Sciences, Durham University, Durham, DH1 3LE, UK.

[2]GEMOC, Department of Earth and Planetary Sciences, Macquarie University, Sydney, NSW 2109, Australia.

[3]School of Physical and Geographical Sciences, Earth Sciences and Geography, Keele University, Keele, ST5 5BG, UK.

*Corresponding author. GEMOC, Department of Earth and Planetary Sciences, Macquarie University, Sydney, NSW 2109 Australia. Telephone: +61 2 9850 4405. Fax: +61 2 9850 8943. Email: heather.handley@mq.edu.au

Abstract

New Nd-Hf isotope and trace element data for Javanese volcanoes are combined with recently published data to place constraints on subduction inputs at the Sunda arc in Indonesia and assess the value of Hf anomalies (expressed as Hf/Hf* and Sm/Hf ratios) as tracers of such inputs. The Hf anomaly does not correlate with Hf isotope ratio in Javanese lavas, however, Hf/Hf* and Sm/Hf ratios do correlate with SiO_2. Contrary to previous work, we show that Hf anomaly variation may be controlled by fractionation of clinopyroxene and/or amphibole during magmatic differentiation and does not represent the magnitude or type of subduction input in some arcs. Correlation of Sm/Hf with indices of differentiation for other arcs (e.g. Vanuatu, New Britain, Mariana) suggests that differentiation control on Sm/Hf ratios in volcanic arc rocks may be a relatively common phenomenon. This study corroborates the use of Nd-Hf isotope co-variations in arc volcanic rocks to ascertain subduction input characteristics. The trajectories of regional volcano groups (East, Central and West Java) in Nd-Hf isotope space reveal heterogeneity in the subducted sediment input along Java, which reflects present-day spatial variations in sediment compositions on the down-going plate in the Java Trench.

1. Introduction

Ascertaining inputs to the mantle wedge in subduction zones is crucial if we are to understand crustal recycling, constrain the geochemical evolution of mantle reservoirs and investigate the fate of subducted sediments. Using the appropriate geochemical tools to ascertain such inputs (slab fluid and/or melt) is therefore of the utmost importance. Several workers have shown that Hf isotope ratios provide great potential to document mantle source compositions and subducted sediment inputs at island arcs (e.g. White and Patchett 1984; Pearce et al., 1999; Woodhead et al., 2001). Hf, as a high field strength element (HFSE), is

thought to behave conservatively, i.e. to have low solubility in aqueous fluids (cf. Woodhead et al., 2001) and should therefore largely avoid transportation to the mantle wedge during dehydration of subducted sediment or crust. Experimental investigations (Tatsumi et al., 1986; Brenan et al., 1995; You et al., 1996; Kessel et al., 2005) and conclusions from other arc studies (McCulloch and Gamble, 1991; Pearce and Peate, 1995; Münker et al., 2004; Turner et al., 2009) suggest that both Nd and Hf are relatively fluid immobile elements (e.g. compared to Sr). Although limited Hf isotope data is available for altered oceanic crust (AOC) to test the immobility of these elements, recent work by Chauvel et al. (2009) has shown that altered basalts from the western Pacific are indistinguishable in their Hf-Nd isotopic ratio compared to unaltered Pacific MORB. This confirms previous suggestions (e.g. White and Patchett, 1984) that hydrothermal alteration has little or no effect on these ratios (cf. Sr isotopes; Staudigel et al., 1995) and, importantly, then affords the opportunity to constrain sedimentary subduction input additions at island arcs.

Hf concentration anomalies of erupted lavas have also been promoted as a tracer of subducted sediment input (e.g. Pearce et al., 1999; Marini et al., 2005; Tollstrup and Gill, 2005). The Hf anomaly is most commonly defined as the relative depletion/enrichment of Hf compared to Nd and Sm on an extended chondrite-normalised rare earth element (REE) diagram (e.g. Pearce et al., 1999). Therefore, the Sm/Hf ratio is suggested by some as the simplest way of quantifying Hf anomalies in arc lavas (e.g. Marini et al., 2005). Using Sm/Hf ratios also enables direct comparison between data sets, avoiding variations produced in Hf anomaly values due to the choice of different normalising factors, e.g. C1 chondrite, depleted mantle MORB (DMM) and primitive mantle (PM). Pearce et al. (1999) calculate Hf anomalies based on Yb-normalised Hf and Nd element ratios to minimise the effects of partial melting and fractional crystallisation. However, the authors indicate that normalisation by Yb is unsuitable if amphibole crystallisation is involved in petrogenesis. As amphibole is

thought to be important in the formation of many arc lavas (e.g. Foden and Green, 1992; Davidson et al., 2007) calculation of Hf anomalies using this method may not be appropriate. Negative Hf anomalies are common in arc lavas, and are interpreted as addition of a subduction component with a high Nd/Hf ratio (Pearce et al., 1999). However, the addition of a sediment component with a low Nd/Hf ratio cannot adequately explain the positive Hf anomalies Pearce et al. (1999) observe in the Izu-Bonin-Mariana Protoarc lavas. In contrast, Salters and Hart (1991) suggested that HFSE variations in arc lavas are not solely due to the addition of a slab-derived component and attribute HFSE depletions to a HFSE-depleted sub-arc mantle reservoir.

Consequently, further research is required to ascertain the use of Hf anomalies as source input indicators. Using new, and recently published (e.g. Handley et al., 2007; 2008a; 2010) Nd-Hf isotope and trace element data from Java, this paper investigates the dominant control on Hf anomaly variation and constrains subducted sediment contributions in Javanese arc lavas. Variations in sediment composition deposited on the down-going plate along the Java Trench provide an ideal location to test whether the heterogeneous nature of sediments in the trench can be tracked in the output of the volcanoes. Identifying whether a homogeneous (as proposed by Edwards et al., 1993) or heterogeneous subduction component is involved in petrogenesis will also help to elucidate the nature of the subduction component in the Sunda arc. Our results emphasise that much greater care needs to be taken, when choosing trace element ratios to determine source component characteristics, by prior consideration of the potential influence of magmatic differentiation processes.

2. Geological Setting and Sample Selection

The island of Java is located in the central section of the Sunda arc, which extends from the Andaman Islands north of Sumatra to Flores in the Banda Sea (Hamilton, 1979, Fig. 1).

Present volcanic activity is related to the northward subduction of the Indo-Australian Plate beneath the Eurasian Plate. The tectonic features of the area are described in depth by Hamilton (1979). Recent work highlighting the structural complexity of the Java crust is detailed in Smyth et al. (2007) and Clements et al. (2009).

Across-arc changes in chemistry are recognised at the Sunda arc (Rittman, 1953; Whitford and Nicholls, 1976; Hutchinson, 1976; Edwards, 1990), therefore, the rear-arc volcanoes of Muriah (370 km above the Wadati-Benioff zone (WBZ) in Central Java) and Ringgit Beser (210 km above the WBZ in East Java) are excluded from data comparison. To ease the recognition of general along-arc contrasts in the large Javanese dataset on bivariate diagrams, volcanoes are grouped into East, Central and West Java provenance based on geographical boundaries. The boundary for Central Java passes between Cereme and Slamet volcanoes in the West and Wilis and Kelut volcanoes in the East (Fig. 1b). Krakatau, in the Sunda Strait (west of Java) is included, accordingly, within the West Java group. A summary of the volcanic data used and source references (Table A.1) and a compilation of major and trace element data for samples with new isotope data (Table A.2) are presented in Appendix A. New Nd-Hf isotope data are presented for Gede Volcanic Complex (GVC) and Guntur in West Java and Merapi in Central Java (Table 1). All new major element, trace element and Sr-Nd isotope data are listed for Merbabu (Central Java) and Merapi in Table 2. See Fig. 1b for the location of volcanoes with new data presented.

Despite unequivocal evidence for the incorporation of a subducted sediment component in other arcs, e.g. from studies of the cosmogenic isotope ^{10}Be (Tera et al., 1986; Morris et al., 1990), it is uncertain whether trench sediments are largely subducted or accreted at the Java Trench. ^{10}Be data from Sunda arc lavas cannot confirm sediment input to the mantle wedge (Edwards et al., 1993), but also do not preclude it. The presence of an accretionary prism in the fore-arc region of the Sunda arc at Java (Kopp et al., 2001) clearly

shows that off-scraping of some proportion of trench sediments occurs. Nevertheless, even where large accretionary prisms are formed at convergent margins, some portion of the sedimentary pile is still thought to be subducted (Westbrook et al., 1988; von Huene and Scholl, 1991; Clift and Vannucchi, 2004). Von Huene and Scholl (1991) assume that 70-80% of the trench sediment is subducted at accretionary margins. Plank and Langmuir (1998) proposed that 300 m of sediment is subducted beneath Java. The sediment type and mass deposited in the trench vary along the arc. Up to 5 km of sedimentary material fills the Sumatra Trench, less than 1 km exists in the western Java Trench and virtually no trench sediments are present in the eastern Java Trench (Plank and Langmuir, 1998). The thicker sedimentary deposits present at the site of subduction in West Java, compared with East Java, are a result of the closer proximity of West Java to turbiditic material sourced from the Himalayan collision zone and deep-sea fans surrounding India (Plank and Langmuir, 1998). Sediments deposited on the Indian Ocean Plate south of the trench are relatively uniform in thickness along the arc (200-400 m) (Hamilton, 1979; Moore et al., 1980; Plank, 1993) and dominantly pelagic (Hamilton, 1979). The large contrast between some element concentrations in sediments and the depleted upper mantle (assumed island-arc magma source), suggests that even a small amount of subducted sediment may exert a large control on the composition of arc lavas. Identification of such contrasts in geochemistry between the arc-mantle source and erupted lavas, which are not a result of magmatic differentiation, are key to answering the question of heterogeneity in the subducted component along Java.

The local Indian Ocean sediments used in geochemical comparisons and modelling (from locations displayed in Fig. 1a), have been broadly grouped as detrital sand-rich, with a high abundance of terrigenous detrital phases (e.g. turbidites), or pelagic clay-rich (e.g. pelagic clay). Despite variation in chemistry for some elements, within each group there are strong links between sediment geochemistry and mineralogy. For example, detrital sand-rich

sediments are generally higher in Zr and Hf (attributed to the higher abundance of zircon) than pelagic clay-rich sediments (e.g. Carpentier et al., 2009).

3. Analytical techniques

For details on the analytical procedures for published data used in this study, refer to the source references in Table A.1. (Appendix A). The new Merapi (M95-028, M96-50 and M96-175) and Merbabu major element, trace element and Sr-Nd isotopic data were collected over the same time period as the Merapi data published in Gertisser and Keller (2003), using the same procedures and data quality constraints given by the authors. Trace element concentrations of Merapi whole-rock powders (M96-102, M98-030 and M98-031) were determined on the PerkinElmer ELAN 6000 quadrupole ICP-MS at Durham University following the analytical procedure and instrument operating conditions described by Ottley et al. (2003). The procedure is the same as that used (during the same time period) for all the Javanese volcanic rock trace element data presented by Handley et al. (2007; 2008a; 2010) used as comparison data in this study. During this period, calibration of the ELAN was achieved during each session via the use of in-house standards and international reference materials: W2, BHVO-1, AGV1, BE-N and BIR1 together with procedural blanks (3 per batch). Accuracy of the analytical method is shown by the agreement of the analyses with international standard data (Table B.1. Appendix B). Total procedural blanks were typically low and maximum blank concentrations (n = 70) are displayed in Table B.1 (Appendix B). Multiple analyses of blanks and standards during each session, e.g. at the start, mid-way, and at the end of a run, allowed any drift in the instrument calibration to be detected. Table B.2 (Appendix B) shows sample reproducibility, measured by replicate analysis of an internal rock standard, KI 202 from Ijen VC over the period of study. Comparisons between XRF (Sitorus, 1990) and ICP-MS (Handley et al., 2007) measurements for Zr are shown in Fig.

B.1 (Appendix B) and display good agreement (R^2 = 0.97) suggesting that dissolution of accessory minerals, such as zircon, was successful during sample preparation for ICP-MS analysis.

Preparation of whole rock powders for Nd and Hf isotope analysis was undertaken in the Arthur Holmes Isotope Geology Laboratory (AHIGL) at Durham University. The sample dissolution procedure and chemical separation of Hf and Nd from rock samples follows that presented by Dowall et al. (2003). Nd and Hf isotope ratios were determined on the AHIGL ThermoElectron Neptune Multi-collector Plasma Mass Spectrometer (MC-ICP-MS). Details of instrument operating conditions are presented in Nowell et al. (2003) and Dowall et al. (2003). Instrumental mass bias was corrected for using a $^{146}Nd/^{145}Nd$ ratio of 2.079143 (equivalent to the more commonly used $^{146}Nd/^{144}Nd$ ratio of 0.7219) and $^{179}Hf/^{177}Hf$ ratio of 0.7325 using an exponential law. Data quality was monitored over several analytical sessions by regular analysis of standard reference materials during each run. The reproducibility of $^{143}Nd/^{144}Nd$ and $^{176}Hf/^{177}Hf$ ratios for the respective standard solutions in each of the individual analytical sessions is better than 19 and 28 ppm (2σ), respectively. The average reproducibility and accuracy of Nd and Hf isotope ratios of standard solutions over the period of study are shown in Table B.3 (Appendix B) For consistency in dataset comparison Nd-Hf isotope data are presented in plots relative to J&M and JMC 475 standard values of 0.511110 (Royse et al., 1998) and 0.282160 (Nowell et al., 1998), respectively. Blank samples processed (at least 2 per sample batch) were analysed by ICP-MS on the PerkinElmer ELAN 6000 quadrupole at Durham University. Total analytical blanks were below 219 pg for Nd and 73 pg for Hf. These values are insignificant considering the quantity of Nd and Hf processed from the volcanic rocks (~5 μg and ~0.9 μg, respectively). Inter-laboratory comparison of Nd isotope analyses for Guntur, comparing the analyses from this study and those by Edwards et al. (1993), are presented in Table B.4 (Appendix B).

4. Results

4.1. Hf concentration anomaly

New major and trace element concentrations of Merapi and Merbabu volcanoes are presented in Table 2. Hf/Hf* is calculated as the relative depletion/enrichment of Hf compared to Nd and Sm on an extended chondrite-normalised rare earth element (REE) plot (Fig. 2). The bracketing elements of Nd and Sm are chosen as they possess peridotite/melt coefficients either side of Hf (e.g. Salters, 1996; Pearce et al., 1999). Fig. 2a shows Hf/Hf* versus $^{176}Hf/^{177}Hf$ isotope ratio for Javanese volcanic rocks. The arc lavas are displaced from Indian Mid-Ocean Ridge Basalt (IMORB), thought to represent the mantle wedge beneath the Sunda arc (e.g. Handley et al., 2007; Gertisser et al., submitted), to lower $^{176}Hf/^{177}Hf$ ratios. Hf/Hf* of the lavas (0.53-1.38) extend to both higher and lower values than IMORB (Hf/Hf* = 0.8-1.2). In contrast to the apparent correlation in Mariana volcanic rocks (Tollstrup and Gill, 2005) no correlation is observed between Hf anomaly or Sm/Hf (inset diagram) and Hf isotopes; the Javanese lavas exhibit a wide range in Hf/Hf* for a relatively small variation in $^{176}Hf/^{177}Hf$ isotopes, particularly for the East Java group (Fig. 2a). Due to the extremely limited Hf isotope data (with accompanying Nd isotope data) available for local Indian Ocean and Java Trench sediments (n = 5), the range of Hf/Hf* of the sediments are indicated along the y-axis. The pelagic, clay-rich sediments display negative Hf/Hf* (<1), while the detrital, sand-rich sediments possess values ≥ 1. Sediment samples for which Hf isotope data are available show that the sand-dominated, turbidite sediments extend to lower $^{176}Hf/^{177}Hf$ isotope ratios than the clay-rich pelagic sediment (and an associated Mn nodule). A noteable observation, previously unmentioned and/or unobserved for other data sets, is that Hf/Hf* in Javanese lavas correlates positively with SiO_2 (Fig. 2b). This feature is explored in detail in section 5.1.

4.2. Hf and Nd isotope variation

New whole-rock Nd-Hf isotope data are given in Table 1 and displayed in Fig. 3. The Javanese volcanic rocks are displaced from IMORB and Pacific- and Atlantic-MORB (other MORB) fields towards lower εNd and εHf, and lie on mixing lines between average IMORB and local sediments from the down-going slab. West Java lavas exhibit a strong positive correlation in Nd-Hf isotope space. Central Java lavas also display a positive correlation but the data are located at higher εHf values for similar εNd values compared to West Java lavas. East Java lavas exhibit somewhat constant εHf and a restricted range in εNd compared to the West Java lavas (Fig. 3b).

5. Discussion

5.1 Hf anomaly variation: 'source' or 'process' control

The lack of correlation between Hf anomaly (Hf/Hf* and Sm/Hf) and Hf isotope ratio, and the correlation of Hf anomaly with SiO_2 in Javanese volcanic rocks (Figs. 2 and 4) strongly suggest that magmatic differentiation at crustal depths may control Hf/Hf* variation. This hypothesis conflicts with recently published discussions, which consider subducted sediment as the dominant control on Hf/Hf* variation in arc rocks (e.g. Marini et al., 2005; Tollstrup and Gill, 2005). The positive correlation of the Java data in Fig. 2b, traverses the line of Hf/Hf* = 1, which suggests the shift between negative to positive Hf anomaly values is related to a single process, and one that commonly occurs in magma genesis at all Javanese volcanoes. Several authors suggest that fractionation between Sm and Hf is negligible, for example during partial melting of fertile mantle and at the early stages of subsequent fractional crystallisation (e.g. Pearce et al., 1999; Chauvel and Blichert-Toft, 2001), such that Sm/Hf may be a good proxy for source composition (e.g. Marini et al., 2005). However, a

literature survey on experimental, theoretical and calculated phenocryst-matrix distribution coefficients (D) in basaltic-andesitic compositions reveals that for several major rock-forming minerals, such as plagioclase, clinopyroxene and amphibole, determined distribution coefficient Sm/Hf ratios ($D_{Sm/Hf}$) are > 1 (e.g. Fig. 4a). Thus, Sm is more compatible than Hf in these minerals and therefore, crystal fractionation of such minerals should lead to decreasing Sm/Hf ratio in the melt with progressive crystal fractionation (and simultaneous modification of Hf anomaly values). Thirwall et al. (1994) suggest a similar control of amphibole and/or clinopyroxene fractionation on Zr/Sm ratios in some Lesser Antilles volcanic rocks. The absolute D values for Sm (and Hf) are low for plagioclase in basalt to andesite compositions, e.g D_{Sm} 0.044-0.11 (Luhr and Carmichael, 1980; Dostal et al., 1983; Fujimaki et al., 1984; Bacon and Druitt, 1988; McKenzie and O'Nions, 1991; Aignertorres et al., 2007) compared to D_{Sm} values of 0.8-1.6 for clinopyroxene (Larson, 1979; Luhr and Carmichael, 1980; Dostal et al., 1983; Fujimaki et al., 1984; Bacon and Druitt, 1988; McKenzie and O'Nions, 1991; Hart and Dunn, 1993; Johnson, 1998) and 0.66-2.221 for amphibole (Luhr and Carmichael, 1980; Dostal et al., 1983; Fujimaki et al., 1984; Bacon and Druitt, 1988; Brenan et al., 1995). Thus, plagioclase fractionation is unlikely to exert as much influence as clinopyroxene and/or amphibole on the Sm/Hf ratio of the remaining melt composition during differentiation. Fig. 4a also shows that $D_{Sm/Hf}$ values are dependent on rock composition, which is particularly evident for clinopyroxene, where $D_{Sm/Hf}$ values progressively increase with increasing silica content.

Fig. 4b shows the strong negative correlation observed between Sm/Hf and SiO_2 for individual volcanic rock suites from Java and the inset diagram also shows the correlation of Sm/Hf with CaO). To investigate whether fractional crystallisation of common mineral phases can explain the Sm/Hf whole rock ratios, a 3-step fractional crystallisation model has been developed using a typical Javanese volcanic rock mineral assemblage, and incorporating

the increase in $D_{Sm/Hf}$ with increasing SiO_2. Step 1: removal of plagioclase, clinopyroxene, magnetite and olivine from KI 63 basalt. Steps 2 and 3: removal of plagioclase, clinopyroxene, magnetite and orthopyroxene from basaltic andesite and andesite, respectively. Full details of modelling parameters (including the *D* values used for each step) are given in the caption to Fig. 4c. For ease of modelling, Sm/Hf ratio, rather than Hf/Hf* is used to represent the Hf anomaly of the lavas. The model reveals the significant control crystal fractionation of a typical mineral assemblage can exert on the Sm/Hf ratios of the volcanic rocks and replicates the general array of the Java data. Variations in model input parameters such as mineral mode and composition, parent whole-rock composition and distribution coefficients also enable more acceptable and less acceptable models to be produced. It is noted that despite the low absolute *D* values for Sm (and Hf) in plagioclase in basalt to andesite compositions, its dominance of the mineral mode in Java volcanic rocks (e.g. Gertisser and Keller, 2003; Handley et al., 2007) enables plagioclase to exert a significant degree of control on model trends (not shown) depending on the particular modal content chosen. The grey shaded area in Fig. 4c shows the relative impact of the choice of partition coefficients for clinopyroxene in Step 3 using the observed range of D_{cpx} values for Sm and Hf given in Fig. 4a for andesitic compositions, which encompasses a range in $D_{Sm/Hf}$ of 2-4. The shaded area shows the wide variation of solutions possible using reasonable sets of distribution coefficients. Fractional crystallisation of a mineral assemblage including clinopyroxene and/or amphibole during magmatic differentiation at Javanese volcanoes is therefore proposed to exert a major control on the Hf anomaly variation of the lavas. Furthermore, the vertical data array observed in Fig. 2a (wide range of Hf/Hf* exhibited by the lavas over a relatively small range in $^{176}Hf/^{177}Hf$) and lack of correlation between Sm/Hf and $^{176}Hf/^{177}Hf$ (Fig. 2a inset) illustrates that the data do not lie on a simple mixing trajectories with subducted sediment (cf. εNd versus εHf; Fig. 3). The magnitude of the

negative Hf anomaly observed in the chemically least evolved rocks (highest MgO, lowest SiO_2 content) may present the best representation of sediment input. However, as most arc rocks are relatively fractionated and have low MgO contents (particularly on Java), even the Sm/Hf ratio of basalt is likely to have undergone some degree of modification due to magmatic differentiation. This is illustrated by Thirlwall et al. (1994) who show that fractional crystallisation (and AFC) have strong effects on HFSE/REE (Zr/Sm) ratios, even in volcanic rocks samples with 6-10 wt% MgO.

Interestingly, a negative correlation between Sm/Hf ratio and the silica content of lavas is also observed in other volcanic arcs (e.g. Vanuatu, New Britain, Mariana, Fig. 4d), suggesting that differentiation control on the Sm/Hf ratio of volcanic rocks may be a relatively common phenomenon. This observation may go some way to explain the observed positive Hf anomalies in more fractionated rock compositions. It may also provide an explanation for the positive Hf anomalies observed in the relatively evolved (up to 67 wt% SiO_2) Protoarc lavas from the Mariana arc investigated by Pearce et al. (1999), as a moderate negative correlation does in fact exist between Sm/Hf and SiO_2 for the Protoarc lavas (Fig. 4d).

5.2. Nd-Hf isotope constraints on source inputs

Contamination of the mantle source by a fluid created during dehydration of the AOC is largely undetectable on plots of εNd-εHf (e.g. Handley et al., 2007). Therefore, displacement of the Java data from the MORB field is likely to be the result of a 'crustal' input during magma genesis (subducted sediment +/- assimilated arc crust). Crustal assimilation has been implicated in the western Sunda arc (Gasparon et al., 1994; Gasparon and Varne, 1998) and on Java (Chadwick et al., 2007; Handley et al., 2008a). Therefore, prior to discussing subducted sediment inputs it is important to assess the potential of crustal assimilation to

modify the isotope ratios. Fig. 5 shows Hf isotope ratio versus SiO_2 (as an index of differentiation) for West, Central and East Java volcanic rocks. The new Hf isotope data are displayed as solid symbols in Figs. 5b and c. Despite the wide variation in $^{176}Hf/^{177}Hf$ isotope ratios exhibited by West Java volcanoes (Fig. 5a), individual volcanic suites from that region display relatively horizontal trends (Fig. 5b) that are inconsistent with significant crustal contamination of isotopically distinct material (inset Fig. 5d, arrows labelled AFC). Less individual volcanic suite data are available for Central and East Java, but for the data available, the absence of correlations between Hf isotope ratios and SiO_2 also preclude significant isotopic modification via crustal assimilation. The Ijen Volcanic Complex in East Java (Fig. 5d) produces lavas with remarkably homogenous Hf isotope ratios over a relatively wide range in SiO_2. This method of assessment naturally assumes that the crustal assimilation is coupled with fractional crystallisation (i.e. AFC, e.g. DePaolo, 1981), and that the fractional crystallisation is responsible for the observed silica range. However, modelling of $\delta^{18}O$ mineral data and $^{87}Sr/^{86}Sr$ whole-rock isotope data also support 'source' contamination rather than a 'crustal' contamination mechanism for the same volcanic rock samples from Gede Volcanic Complex, Salak volcano and Ijen Volcanic Complex (Handley et al., 2010).

Incorporation of a subducted component in the mantle source dominated either by clay- or sand-rich local sediment will produce very different mixing trends in Nd-Hf isotope space due to the contrasting Nd/Hf ratios of the sediments (e.g. Patchett et al., 1984; Carpentier et al., 2009). Pelagic, clay-rich Indian Ocean sediments have variable and relatively high Nd/Hf (6-42, n = 9, Plank and Langmuir, 1998; Ben Othman et al., 1989; Gasparon and Varne, 1998) resulting in convex-up mixing trends towards higher εHf relative to εNd, whereas continentally derived detrital/sand-rich local sediments tend to have relatively low Nd/Hf (4-7, n = 6, Ben Othman et al., 1989; Vervoort et al., 1999; Gasparon and Varne, 1998) producing relatively straight mantle source-sediment mixing curves,

associated with lower εHf relative to εNd (Fig. 3a inset). Therefore, we can examine whether the different isotopic arrays exhibited by separate geographical groups on Java reflect variations in the composition of subducting sediment. Simple bulk-mixing calculations between average IMORB mantle source and pelagic clay (curve B) and sand-rich turbidite (curves C and D) sediments are presented in Figs. 3a and b. Due to the lack of local sediment Nd-Hf isotope data (n = 5) a mixing curve using Mn nodule (Curve A) was also calculated to further exemplify mixing with high Nd/Hf and 'pelagic' Nd-Hf isotope composition material. We acknowledge that Mn nodules are unlikely to represent the entire subducting sedimentary section at the Java Trench. However, recent work by Chauvel et al. (2009) shows that almost all pelagic sediment types (chert, clay and carbonate lithologies) at drill Site 1149 in the western Pacific plot within the Fe-Mn crusts and nodule field in εNd-εHf isotope space, supporting the use of a Mn nodule to represent that of pelagic sediment. The end member compositions used in modelling are displayed in Table 3. The mixing curves suggest that displacement of Javanese arc lavas from IMORB εNd and εHf ratios and domain trajectories can be explained by addition of a small amount (generally < 5 %) of turbidite-dominated, sand-rich, low Nd/Hf sedimentary material to the mantle source of West Java lavas, and addition of a similar-sized, sedimentary component dominated by pelagic clay-rich, higher Nd/Hf material to the mantle source of Central Java lavas. The limited spread of the East Java field is largely due to the lack of Nd-Hf isotope data from other volcanoes except Ijen Volcanic Complex (one sample from both Semeru and Lamongan, Fig. 3b). The Ijen data lie on the detrital-rich sediment-mantle source mixing lines. However, an alternative solution was proposed by Handley et al. (2007), who show that Sr-Nd-Hf isotope data trends are consistent with mixing of high Nd/Hf sediment with a mantle-wedge source composition of slightly lower than average IMORB Hf isotope ratio (Fig. 3b inset). This is further supported by new Nd-Hf isotope data for Tambora volcano (Gertisser et al., submitted), located to the

east of Java (Fig. 1a), where the subducting sediment is also proposed to be clay-dominated (e.g. DSDP site 261). The Tambora data display a relatively horizontal array (cf. West Java); showing significant range in εNd over a limited range in εHf (Fig. 3b inset), consistent with mantle source contamination by high Nd/Hf sediment. This interpretation of Javanese volcanic rock data is consistent with the greater amount of continentally-derived, detrital-rich turbidite sediment observed in the trench opposite West Java compared to Central and East Java, due to the closer proximity of West Java to the Himalayan/Ganges turbidite source.

We recognise that subducted sediment is more likely to be added to the mantle wedge as a partial melt rather than as a bulk component (as modelled here). However, due to the many assumptions required in order to calculate a partial melt composition (such as sediment composition and residual mineralogy, degree of melting, depth of melting, thermal conditions of the melting region and appropriate distribution coefficients), we use bulk-mixing models to illustrate the broad effects of mantle-sediment mixing. Partial melting of sediment with residual phases such as zircon is likely to increase the Nd/Hf ratio of the sediment component. However, this increase would be offset by the presence of residual monazite which is suggested to have D_{Hf} 4-5 orders of magnitude lower than D_{Sm} and thereby lowering the Nd/Hf ratio of the sediment-melt (Tollstrup and Gill, 2005 and references therein). Ultimately, partial melting of sediment is likely to reduce the percentage of subducted sediment suggested by bulk-mixing models.

5.3. Implications for magma genesis in the Sunda arc

Gasparon and Varne (1998) argue that crustal assimilation, opposed to subducted slab input, is the dominant process responsible for the isotopic and geochemical variability and "enrichment" along the Sunda arc. Despite field evidence of crustal anatectic melts in Sumatra and West Java (Hamilton, 1979; Gasparon and Varne, 1995) and more recently

implicated crustal contamination at Salak (Handley et al., 2008a) and Merapi (Chadwick et al., 2007), findings from this study suggest the dominant geochemical control on Nd-Hf isotope and some trace element characteristics occurs through subducted slab input to the mantle wedge followed by subsequent evolution through magmatic differentiation, largely excluding crustal contamination. Addition of a subducted slab component to the Sunda arc mantle wedge is advocated by several other authors (e.g. Edwards, 1990; Turner and Foden, 2001; Gertisser and Keller, 2003; Handley et al., 2007, 2010), although Edwards et al. (1993) propose a homogeneous slab contribution along the Sunda arc. We attribute the different trajectories of Javanese volcanic groups in Nd-Hf isotope space to the incorporation of a heterogeneous subduction component, which largely reflects spatial variations observed in present day sediment types deposited on the down-going plate along the Java Trench (Fig. 3). A positive correlation in Nd-Hf isotope space for West Java volcanic rocks is consistent with the incorporation of a dominantly continental-derived, detrital-rich sedimentary component, whereas, the arrays of volcanic data in Nd-Hf isotope space for Central and East Java volcanoes are consistent with a more pelagic, clay-rich subducted sedimentary component and possibly stronger slab-fluid imprint, as concluded for Ijen Volcanic Complex (Handley et al., 2007). The along arc variation in sediment type proposed in magma genesis is consistent with the decreasing thickness of turbidite deposits in the trench from Sumatra to East Java.

The tholeiitic basalts from Guntur display some of the least sediment-contaminated Nd-Hf isotope ratios, despite being located in West Java where the thickest sediment pile is present in the adjacent trench (cf. Central/East Java). Guntur volcano sits within a fault-bound tectonic triangle (e.g. Soeria-Atmadja et al., 1994) where the crust may be thinner and decompression melting (cf. slab-fluxing) may be important in magma genesis (Handley, 2006). Mafic glass inclusion data from neighbouring Galunggung volcano show that

pressure-release melting of the mantle wedge contributes to magma production within this region (Sisson and Bronto, 1998).

The required along-arc heterogeneity in the subduction component along the Sunda arc, restricts the applicability of modelling slab inputs using a 'bulk composition' sediment approach. The bulk Java subducted sediment composition calculated by Plank and Langmuir (1998) does not produce an acceptable mixing array with the mantle wedge to fit the data array of from either East or West Java volcanic centres (Handley et al., 2007). Combining our results with those of Vroon (1992) and Vroon et al. (1995) for sediments and volcanic rocks of the Banda arc (East Indonesia), heterogeneity in the recycled subduction component can now be traced along most of the Indonesian arc. In the west Sunda arc we see the importance of detrital-rich, terrigenous subducted sediments (of Himalayan/Ganges source), which moving eastwards, changes to dominantly pelagic sediment in the central and eastern Sunda arc region e.g. East Java and Sumbawa (Tambora; Gertisser et al., submitted). Further east at the Banda arc, we see a return to the involvement of detrital-rich terrigenous sediment and a larger degree of mantle contamination moving from northeast to southwest, corresponding to increasing fluxes of continental material into the trench towards the sector where the collision between Australia and the Banda arc began.

6. Conclusions

This study highlights and corroborates the importance of Hf and Nd isotopes as petrogenetic tools for identifying and characterising sediment subduction in arc volcanic rocks. However, contrary to previous interpretations, Hf anomalies may not represent subduction input in some arcs, particularly the Sunda arc. We show it is possible to create significant variation in Hf anomaly through fractional crystallisation involving clinopyroxene and/or amphibole as the major mafic mineral phases. Subsequently, it may not be appropriate to use Sm/Hf in

volcanic rocks as a proxy for magmatic source composition without prior consideration of differentiation control. Source studies of island arcs often neglect to assess the impact of magmatic differentiation effects prior to source input evaluation, however, we re-emphasise in this paper that it must be a prerequisite. This study also presents a potential implication for melting in the presence of a clinopyroxene-rich residue, which may also affect calculated Hf anomalies in arc lavas. A preliminary investigation of Sm/Hf variation with SiO_2 for other arcs suggests that Sm/Hf fractionation via differentiation processes is a ubiquitous feature of arc magmas.

New Nd-Hf isotopic and trace element data of Sunda arc volcanoes reveal significant heterogeneity in the subduction component along the Sunda arc. This is attributed to incorporation of subducted sediment, the composition of which is controlled by observed spatial variations in the sediments deposited on the down-going Indian Ocean plate. Due to significant heterogeneity in the subduction input along Java, using an average 'bulk-sediment' to represent the subduction component for the whole arc is, therefore, unsuitable.

Acknowledgements

We would like to thank Akhmad Zaennudin and his colleagues at the Volcanic Survey of Indonesia in Bandung for invaluable logistical help and guidance in the field. Geoff Nowell and Chris Ottley at Durham University are thanked for technical support and analytical assistance. Simon Suggate and Helen Smyth compiled the Digital Elevation Model map of Java from SRTM data. Robert Hall provided samples for Guntur. The manuscript significantly benefited from the editorial comments of Richard Carlson and reviews by Catherine Chauvel and Matthew Thirlwall. Sample collection and analysis were supported by a NERC studentship (NER/S/A/2001/06127) and the SEARG at Royal Holloway University of London. S.T. acknowledges the support of Australian Research Council Federation and

Professorial Fellowships. This is contribution 703 from the Australian Research Council National Key Centre for the Geochemical Evolution and Metallogeny of Continents (http://www.gemoc.mq.edu.au).

Figure Captions

Fig. 1. a) Schematic illustration of the tectonic features of the Sunda arc. Open squares indicate the location of Indian Ocean sediment drill and dredge sites (taken from Gasparon and Varne (1998) and Vroon (1992)). The suggested southeast limit of terrigenous turbidite deposits in the trench is also shown (Hamilton, 1979). b) Map of Java showing volcano location. The volcanoes for which new geochemical and isotopic data are presented in this study (Gede Volcanic Complex, Guntur, Merapi and Merbabu) are shown in bold. Krakatau is not shown (immediately west of West Java). The two white lines in north-south orientation indicate the geographical boundaries of West, Central and East Java. The Digital Elevation Model of Java is complied from SRTM data (Shuttle Radar Topography Mission, NASA data).

Fig. 2. a) Hf concentration anomaly (Hf/Hf*) variation with $^{176}Hf/^{177}Hf$ isotope ratio for Javanese volcanic rocks. The average $^{176}Hf/^{177}Hf$ 2σ error (± 0.000010) is smaller than the symbol size. Hf/Hf* is calculated using the equation: $[(Hf/Hf_N)/[(Sm/Sm_N)+(Nd/Nd_N)/2]$. Normalising values for C1 chondrite are taken from McDonough and Sun, 1995. See Table A.1 (Appendix A) for Java volcanic data sources. Clay-rich sediment data: White et al. (1986); Ben Othman et al. (1989); Plank and Langmuir (1998); Gasparon and Varne (1998) Detrital, sand-rich sediment data: the same references as those for clay-rich sediment plus Vervoort et al. (1999). IMORB data: Salters (1996); Chauvel and Blichert-Toft, (2001). The inset diagram shows Sm/Hf versus $^{176}Hf/^{177}Hf$ isotope ratio for Javanese volcanic rocks. b)

Hf/Hf* versus SiO_2 for Java volcanic rocks. Inset diagram shows the relative enrichment (Hf/Hf* >1) or depletion (Hf/Hf* <1) of Hf relative to Nd and Sm on an extended chondrite-normalised REE diagram. Java data sources are given in Table A.1 (Appendix A).

Fig. 3. a) εHf-εNd diagram showing displacement of Javanese volcanic rocks from the IMORB and other MORB (Pacific and Atlantic) fields. Bulk-mixing models between IMORB source and local high Nd/Hf (15-33) sediment (curves A & B), and local low Nd/Hf (6-7) sediment (curves, C and D) are displayed. A = Mn nodule (V34-62, White et al., 1986; Ben Othman et al., 1989), B = pelagic clay (V34-45, White et al., 1986; Ben Othman et al., 1989) C and D = deep-sea turbidite sediments V28-357-M (CA30-M) and V28-357-M (CA30-S), respectively (Vervoort et al., 1999). End member compositions are given in Table 3. Sediment sample locations are shown in Fig. 1a. Java data fields are distinguished by geographical region and data sources are given in Table A.1 (Appendix A). Inset: A schematic illustration of the mixing curves produced from mixing 'sand-rich' low Nd/Hf sediments and 'clay-rich' high Nd/Hf sediments with a MORB-like mantle source. b) A close up view of the εHf-εNd diagram shown in *a* with the individual fields of Javanese volcanic suites displayed. Mantle-sediment mixing as in *a*. Inset: εHf-εNd diagram illustrating mixing curves produced between three IMORB source compositions with lower than average $^{176}Hf/^{177}Hf$ isotope ratios (MD37-05-02, Chauvel and Blichert-Toft, 2001; 54R-1, 115-121, Nowell et al., 1998; MD34 D2, Chauvel and Blichert-Toft, 2001) and sediment A, modified from Handley et al., 2007. The Tambora data are from Gertisser et al. (submitted).

Fig. 4. a) Distribution coefficients (*D*) of Sm and Hf for basaltic-andesitic rock compositions taken from the literature. Note that in all cases $D_{Sm/Hf} > 1$. Clinopyroxene: Larsen (1979); Luhr and Carmichael (1980); Dostal et al. (1983); Fujimaki et al. (1984); Bacon and Druitt

(1988); McKenzie and O'Nions (1991); Hart and Dunn (1993); Johnson (1998). Amphibole: Luhr and Carmichael (1980); Dostal et al. (1983); Fujimaki et al. (1984); Bacon and Druitt (1988); Brenan et al. (1995). b.a. = basaltic andesite. b) Sm/Hf versus SiO_2 showing a coherent negative correlation for Javanese volcanic rocks and for all individual volcanic suites. Volcanoes with 3 or less data points (Krakatau, Tangkubahn Parahu, Papandayan, Sumbing, Semeru and Lamongan) are plotted but have not been delimited. Inset diagram: Sm/Hf versus SiO_2 showing the Sm/Hf ratios of local sediment (for data sources see Fig. 1a caption). c) Sm/Hf versus SiO_2 of Javanese volcanic rocks showing model fractionation curves for the removal of a typical Java mineral assemblage of plagioclase, clinopyroxene, magnetite plus olivine or orthopyroxene from Ijen Volcanic Complex basalt (KI 63). Step 1 ($D_{bulk(basalt)}$): removal of plag (0.72), cpx (0.18), ol (0.05) and mag (0.05) using D values: plag: Sm, 0.11; Hf, 0.01 (McKenzie and O'Nions, 1991); cpx: Sm, 0.239; Hf, 0.2 (Johnson, 1998); ol: Sm, 0.0049; Hf, 0.0038 (Fujimaki et al., 1984); mag: Sm, 0.29; Hf, 0.30 (Luhr and Carmichael, 1980). Steps 2 ($D_{bulk(b.a.)}$) and 3 ($D_{bulk(andesite)}$): removal of plag (0.7), cpx (0.17), opx (0.09) and mag (0.04) using D values: plag: Sm, 0.1024; Hf, 0.0151 (Fujimaki et al., 1984); opx: Sm, 0.0278; Hf, 0.0508 (Fujimaki et al., 1984); mag: Sm, 0.29; Hf, 0.30 (Luhr and Carmichael, 1980); cpx step 2: Sm, 0.8; Hf, 0.3 (Dostal et al., 1983); cpx step 3: Sm, 1.3; Hf, 0.34 (Luhr and Carmichael, 1980). Grey shaded field exemplifies the possible range in model solutions produced due to variations in D_{cpx} Sm and Hf chosen for Step 3. $D_{Sm/Hf\ (cpx)}$ = 2 uses D_{cpx} Sm, 0.3774; Hf, 0.1730 (Fujimaki et al., 1984); $D_{Sm/Hf\ (cpx)}$ = 4 uses D_{cpx} Sm, 1.6; Hf, 0.46 (Bacon and Druitt, 1998). Whole-rock and mineral compositions are taken from Handley et al. (2007). Tick marks on fractionation curves are given for 10% increments. The Sm/Hf ratios of IMORB use data from Price et al. (1986), Salters (1996) and Chauvel and Blichert-Toft (2001). Inset: Sm/Hf versus CaO for Javanese volcanic rocks. Data sources are shown in Table A.1 (Appendix A). d) Sm/Hf variation with SiO_2 for other volcanic arc rocks.

Vanuatu: Peate et al. (1997); Handley et al. (2008b). Mariana: Woodhead et al. (2001); Elliott et al. (1997); Pearce et al. (1999). Lesser Antilles: Woodhead et al., 2001; Turner et al. (1996); Davidson et al. (1993); Heath et al. (1998). New Britain: Woodhead et al. (2001). Depleted MORB mantle (DMM) from Workman and Hart (2005).

Fig. 5. a) $^{176}Hf/^{177}Hf$ variation with SiO_2 for Javanese volcanic rocks separated by geographic region. b), c) and d) show $^{176}Hf/^{177}Hf$ variation with SiO_2 for individual volcanic suites of West, Central and East Java, respectively. New data is displayed as solid symbols, previously published data is shown by open symbols. Arrows labelled SH, AFC and FC in *d* indicate the hypothesised data trends related to: mantle source heterogeneity (SH), combined assimilation and fractional crystallisation (AFC) and fractional crystallisation (FC). AFC trends can be positive or negative depending on the Hf isotope ratio of the assimilated material. The field for Gede Volcanic complex is divided in two due to the large difference in Hf isotopic composition of the Older Quaternary Volcanic group (2 samples at significantly higher $^{176}Hf/^{177}Hf$), situated to the east of the main Gede Complex (Handley et al., 2010). The low $^{176}Hf/^{177}Hf$ Merapi data point is from Woodhead et al. (2001). Data sources are shown in Table A.1 (Appendix A).

References

Aignertorres, M., Blundy, J., Ulmer, P. and Pettke, T., 2007. Laser Ablation ICPMS study of trace element partitioning between plagioclase and basaltic melts: an experimental approach. Contrib. Mineral. Petrol. 153, 647-667.

Bacon, C.R., Druitt, T.H., 1988. Compositional Evolution of the Zoned Calcalkaline Magma Chamber of Mount-Mazama, Crater Lake, Oregon. Contrib. Mineral. Petrol. 98, 224-256.

Ben Othman, D.B., White, W.M., Patchett, J., 1989. The geochemistry of marine sediments, island arc magma genesis, and crust-mantle recycling. Earth Planet. Sci. Lett. 94, 1-21.

Brenan, J., Shaw, H.F., Phinney, D.L., Ryerson, J.F., 1995. Mineral-aqueous fluid partitioning of trace elements at 900°C and 2.0 Gpa: Constraints on the trace element geochemistry of mantle and deep crustal fluids. Geochim. Cosmochim. Acta 59, 3331-3350.

Bouvier, A., Vervoort, J.D., Patchett, P.J., 2008. The Lu-Hf and Sm-Nd isotopic composition of CHUR: Constraints from unequilibrated chondrites and implications for the bulk composition of terrestrial planets. Earth Planet. Sci. Lett. 273, 48-57.

Carn, S.A., Pyle, D.M., 2001. Petrology and geochemistry of the Lamongan Volcanic Field, East Java, Indonesia: Primitive Sunda Arc magmas in an extensional tectonic setting? J. Petrol. 42, 1643-1683.

Carpentier, M., Chauvel, C., Maury, R.C., Mattielli, N., 2009. The "zircon effect" as recorded by the chemical and Hf isotopic compositions of Lesser Antilles forearc sediments. Earth Planet. Sci. Lett. 287, 86-99.

Chadwick, J.P., Troll, V.R., Ginibre, C., Morgan, D., Gertisser, R., Waight, T.E., Davidson, J.P., 2007. Carbonate Assimilation at Merapi Volcano, Java, Indonesia: Insights from Crystal Isotope Stratigraphy. J Petrol 48, 1793-1812.

Chauvel, C., Blichert-Toft, J., 2001. A hafnium isotope and trace element perspective on melting of the depleted mantle. Earth Planet. Sci. Lett. 190, 137-151.

Chauvel, C., Marini, J.C., Plank, T., Ludden, J.N., 2009. Hf-Nd input flux in the Izu-Mariana subduction zone and recycling of subducted material in the mantle. Geochem. Geophys. Geosystems 10, Q01001, doi:10.1029/2008GC002101.

Claproth, R., 1988. Petrography and geochemistry of volcanic rocks from Ungaran, Central Java, Indonesia. Unpublished PhD Thesis. University of Wollongong, Australia.

Clements, B., Hall, R., Smyth, H.R., Cottam, M.A., 2009. Thrusting of a volcanic arc: a new structural model for Java. Petrol. Geosci. 15, 159-174.

Clift, P.D., Vannucchi, P. 2004. Controls on tectonic accretion versus erosion in subduction zones: Implications for the origin and recycling of the continental crust, Rev. Geophys. 42, RG2001, doi:10.1029/2003RG000127.

Davidson, J.P., Boghossian, N.D., Wilson M., 1993. The geochemistry of the igneous rock suite of St. Martin, Northern Lesser Antilles. J. Petrol. 34, 839-866.

Davidson, J.P., Hora, J.M., Garrison, J.M., Dungan, M.A., 2005. Crustal Forensics in Arc Magmas. J. Volcanol. Geotherm. Res. 140, 157-170

Davidson, J., Turner, S., Handley, H., Macpherson, C., Dosseto, A., 2007. Amphibole "sponge" in arc crust? Geology 35, 787-790.

DePaolo, D.J., 1981. Trace element and isotopic effects of combined wallrock assimilation and fractional crystallization. Earth Planet. Sci. Lett. 53, 189-202.

Dostal, J., Dupuy, C., Carron, J.P., Dekerneizon, M.L., Maury, R.C., 1983. Partition-Coefficients of Trace-Elements - Application to Volcanic-Rocks of St-Vincent, West-Indies. Geochim. Cosmochim. Acta 47, 525-533. doi: 10.1016/0016-7037(83)90275-2.

Dowall, D.P, Nowell, G.M., Pearson, D.G., 2003. Chemical pre-concentration procedures for high-precision analysis of Hf-Nd-Sr isotopes in geological materials by plasma ionisation multi-collector mass spectrometry (PIMMS) techniques. Plasma Source Mass Spectrometry. Spec.Pub. Royal Soc. Chem., 321-337.

Edwards, C.M.H., 1990. Petrogenesis of tholeiitic, calc-alkaline and alkaline volcanic rocks, Sunda arc, Indonesia. Unpublished Ph.D. Thesis, Royal Holloway, University of London, UK.

1 Edwards, C.M.H., Morris, J.D., Thirlwall, M.F., 1993. Separating mantle from slab
2 signatures in arc lavas using B/Be and radiogenic isotope systematics. Nature 362, 530-
3 533.
4 Elliott T.R., Plank T., Zindler A., White W., Bourdon B., 1997. Element transport from slab
5 to volcanic front at the Mariana arc. J. Geophys. Res. B102, 14991-15019.
6 Foden, J., Green, D.H., 1992. Possible role of amphibole in the origin of andesite: some
7 experimental and natural evidence. Contrib. Mineral. Petrol. 109, 479-493.
8 Fujimaki, H., Tatsumoto, M., Aoki, K.-i., 1984. Partition coefficients of Hf, Zr, and REE
9 between phenocrysts and groundmasses. J. Geophys. Res. 89, 662-672.
10 Gasparon, M., Hilton, D.R., Varne, R., 1994. Crustal contamination processes traced by
11 helium isotopes: examples from the Sunda arc, Indonesia. Earth Planet. Sci. Lett. 126,
12 15-22.
13 Gasparon, M., Varne, R., 1995. Sumatran granitoids and their relationship to Southest Asian
14 terranes. Tectonophysics 251, 277-299.
15 Gasparon, M., Varne, R., 1998. Crustal assimilation versus subducted sediment input in west
16 Sunda arc volcanics: an evaluation. Mineral. Petrol. 64, 89-117.
17 Gertisser R., 2001. Gunung Merapi (Java, Indonesien): eruptionsgeschichte und magmatische
18 evolution eines hochrisiko-vulkans. Ph.D. Thesis, Universität Freiburg.
19 Gertisser, R., Keller, J., 2003. Trace element and Sr, Nd, Pb and O isotope variations in
20 medium-K and high-K volcanic rocks from Merapi Volcano, Central Java, Indonesia:
21 evidence for the involvement of subducted sediments in Sunda Arc magma genesis. J.
22 Petrol. 44, 457-489.
23 Gertisser, R., Self, S., Thomas, L. Handley, H., van Calsteren, P., Wolff, J. (submitted).
24 Magma Generation Processes and Timescales Leading to the Great Tambora Eruption
25 in 1815. J. Petrol.

Gerbe, M.-C., Gourgaud, A., Sigmarsson, O., Harmon, R.S., Joron, J-L., Provost, A., 1992. Mineralogical and geochemical evolution of the 1982-1983 Galunggung eruption (Indonesia). Bull. Volc. 54, 284-298.

Hamilton, W.B., 1979. Tectonics of the Indonesian region. U.S. Geological Survey Professional Paper 1078.

Handley, H.K., 2006. Geochemical and Sr-Nd-Hf-O isotopic constraints on volcanic petrogenesis at the Sunda arc, Indonesia. PhD thesis, Durham University.

Handley, H.K., Macpherson, C.G., Davidson, J.P., Berlo, K., Lowry, D., 2007. Constraining fluid and sediment contributions to subduction-related magmatism in Indonesia: Ijen Volcanic Complex, Indonesia. J. Petrol. 48, 1155-1183.

Handley, H.K., Davidson, J.P., Macpherson, C.G., 2008a. Untangling differentiation in arc lavas: constraints from unusual minor and trace element variations at Salak Volcano, Indonesia. Chem. Geol. 255, 360-376.

Handley, H.K., Turner, S.P., Smith, I.E., Stewart, R.B., Cronin, S.J., 2008b. Rapid timescales of differentiation and evidence for crustal contamination at intra-oceanic arcs: geochemical and U-Th-Ra-Sr-Nd isotopic constraints from Lopevi volcano, Vanuatu, SW Pacific. Earth Planet. Sci. Lett. 273, 184-194.

Handley, H.K., Macpherson, C.G., Davidson, J.P., 2010. Geochemical and Sr-O isotopic constraints on magmatic differentiation at Gede Volcanic Complex, West Java, Indonesia. Contrib. Mineral. Petrol. 159, 885-908.

Hart, S.R., Dunn, T., 1993. Experimental cpx/melt partitioning of 24 trace elements. Contrib. Mineral. Petrol. 113, 1-8.

Hartono, U., 1995. The petrology and geochemistry of the Wilis and Lawu volcanoes, east Java, Indonesia. Unpublished PhD Thesis, University of Tasmania, Australia.

Heath, E., Macdonald, R., Belkin, H., Hawkesworth, C.J., Sigurdsson H., 1998. Magmagenesis at Soufriere Volcano, St. Vincent, Lesser Antilles arc. J. Petrol. 39, 1721-1764.

Hutchinson, C.S., 1976. Indonesian active volcanic arc: K, Sr and Rb variation with depth to the Benioff zone. Geology 4, 407-408.

Johnson, K.T.M., 1998. Experimental determination of partition coefficients for rare earth and high-field-strength elements between clinopyroxene, garnet, and basaltic melt at high pressures. Contrib. Mineral. Petrol. 133, 60-68.

Kessel, R., Schmidt, M.W., Ulmer, P., Pettke, T., 2005. Trace element signature of subduction-zone fluids, melts and supercritical liquids at 120-180 km depth. Nature 437, 724-727.

Kopp, H., Flueh, E.R., Klaeshen, D., Bialas, J., Reichert, C., 2001. Crustal structure of the Sunda margin at the onset of oblique subduction. Geophys. J. Int. 147, 449-474.

Larsen, L.M., 1979. Distribution of REE and Other Trace-Elements between Phenocrysts and Peralkaline Undersaturated Magmas, Exemplified by Rocks from the Gardar Igneous Province, South Greenland. Lithos 12, 303-315.

Luhr, J.F., Carmichael, I.S.E., 1980. The Colima volcanic complex, Mexico. I: post-caldera andesites from Volcan Colima. Contrib. Mineral. Petrol. 71, 343-372.

Mandeville, C.W., Carey, S., Sigurdsson, H., 1996. Magma mixing, fractional crystallisation and volatile degassing during the 1883 eruption of Krakatau volcano, Indonesia. J. Volcanol. Geotherm. Res. 74, 243-274.

Marini, J.C., Chauvel, C., Maury, R.C., 2005. Hf isotope compositions of northern Luzon arc lavas suggest involvement of pelagic sediments in their source. Contrib. Mineral. Petrol. 149, 216-232.

McDonough, W.F., Sun, S.-s., 1995. The composition of the Earth. Chem. Geol. 120, 223-253.

McKenzie, D., O'Nions, R.K., 1991. Partial melt distributions from inversion of rare Earth element concentrations. J. Petrol. 32, 1021-1091.

McCulloch, M.T., Gamble J.A., 1991. Geochemical and geodynamical constraints on subduction zone magmatism. Earth Planet. Sci. Lett. 102, 358-374.

Moore, G.F., Curray, J.R., Moore, D.G., Karig, D.E., 1980. Variations in geologic structure along the Sunda fore arc, Northeastern Indian Ocean. In: The Tectonic and Geologic Evolution of Southeast Asian Seas and Islands, ed. Hayes, D., Geophys. Monogr., 23, 145-160.

Morris, J.D., Leeman, W.P., Tera, F., 1990. The subducted component in island arc lavas: constraints from Be isotopes and B-Be systematics. Nature 344, 31-36.

Münker, C., Worner, G., Yogodzinski, G., Churikova, T., 2004. Behaviour of high field strength elements in subduction zones: constraints from Kamchatka-Aleutian arc lavas. Earth Planet. Sci. Lett. 224, 275-293.

Nowell, G.M., Kempton, P.D., Noble, S.R., Fitton, J.G., Saunders, A.D., Mahoney, J.J., Taylor, R.N., 1998. High precision Hf isotope measurements of MORB and OIB by thermal ionisation mass spectrometry: insights into the depleted mantle. Chem. Geol. 149, 211-233.

Nowell, G.M, Pearson, D.G, Ottley, C.J., Schweiters, J., 2003. Long-term performance characteristics of a plasma ionisation multi-collector mass spectrometer (PIMMS): the ThermoFinnigan Neptune. Plasma Source Mass Spectrometry. Spec. Pub. Royal Soc. Chem., 307-320.

Ottley, C.J, Pearson, D.G., Irvine, G.J., 2003. A routine method for the dissolution of geological samples for the analysis of REE and trace elements via ICP-MS. Plasma Source Mass Spectrometry. Spec. Pub. Royal Soc. Chem., 221-230.

Patchett, P.J., White, W.M., Feldmann, H., Kielinczuk, S., Hofmann, A.W., 1984. Hafnium/rare earth element fractionation in the sedimentary system and crustal recycling into the Earth's mantle. Earth Planet. Sci. Lett. 69, 365-378.

Pearce, J.A., Kempton, P.D., Nowell, G.M., Noble, S.R., 1999. Hf-Nd Element and Isotope Perspective on the Nature and Provenance of Mantle and Sunduction Components in Western Pacific Arc-Basin Systems. J. Petrol. 40, 1579-1611.

Pearce, J.A., Peate, D.W., 1995. Tectonic implications of the composition of volcanic arc magmas. Ann. Rev. Earth Planet. Sci. 24, 251–285.

Plank, T., 1993. Mantle melting and crustal recycling at subduction zones. Ph.D. thesis. Columbia University, New York.

Plank, T., Langmuir, C.H., 1998. The chemical composition of subducting sediment and its consequences for the crust and mantle. Chem. Geol. 145, 325-394.

Rittman, A., 1953. Magmatic character and tectonic position of the Indonesian volcanoes. Bull. Volcanol. 14, 45-58.

Royse, K., Kempton, P.D., Darbyshire, D.P.F., 1998. NERC Isotope Geosciences Laboratory Report Series, 121.

Salters, V.J.M., 1996. The generation of mid-ocean ridge basalts from the Hf and Nd isotope perspective. Earth Planet. Sci. Lett. 141, 109-123.

Salters, V.J.M., Hart, S.R. 1991. The mantle sources of ocean islands and arc basalts: the Hf isotope connection. Earth Planet. Sci. Lett. 104, 364-380.

Sissons, T.W., Bronto, S., 1998. Evidence for pressure-release melting beneath magmatic arcs from basalt at Galunggung, Indonesia. Nature 391, 883-886.

Sitorus, K., 1990. Volcanic stratigraphy and geochemistry of the Idjen Caldera Complex, East Java, Indonesia. MSc thesis, University of Wellington, New Zealand.

Smyth, H.R., Hamilton, P.J., Hall, R., Kinny, P.D., 2007. The deep crust beneath island arcs: Inherited zircons reveal a Gondwana continental fragment beneath East Java, Indonesia. Earth Planet. Sci. Lett. 258, 269-282.

Soeria-Atmadja, R., Maury, R.C., Bellon, H., Pringgoprawiro, H., Polve, M., Priadi, B., 1994. Tertiary magmatic belts in Java. J. Southeast Asian Earth Sci. 9, 13-27.

Staudigel, H., Davies, G.R., Hart, S.R., Marchant, K.M., Smith, B.M., 1995. Large scale isotopic Sr, Nd and O isotopic anatomy of altered oceanic crust: DSDP/ODP sites 417/418. Earth Planet. Sci. Lett. 130, 169-185.

Tatsumi, Y., Hamilton, D.L., Nesbitt, R.W., 1986. Chemical characteristics of fluid phase released from a subducted lithosphere and origin of arc magmas: evidence from high-pressure experiments and natural rocks. J. Volcanol. Geotherm. Res. 29, 293-309.

Tera, F., Brown, L., Morris, J., Sacks, I.S., Klein, J., Middleton, R., 1986. Sediment incorporation in island-arc magmas: inferences from ^{10}Be. Geochim. Cosmochim. Acta, 50, 535-550.

Thirlwall, M.F., Smith, T.E., Graham, A.M., Theodorou, N., Hollings, P., Davidson, J.P., Arculus, R.J., 1994. High Field Strength Element Anomalies in Arc Lavas: Source or Process? J. Petrol., 35, 819-838. doi:10.1093/petrology/35.3.819

Tollstrup, D.L., Gill, J.B., 2005. Hafnium systematics of the Mariana arc: evidence for sediment melt and residual phases. Geology 33, 737-740.

Turner, S., Foden. J., 2001. U, Th and Ra disequilibria, Sr, Nd and Pb isotope and trace element variations in Sunda arc lavas: predominance of a subducted sediment component. Contrib. Mineral. Petrol. 142, 43-57.

Turner S.P., Hawkesworth C.J., van Calsteren P., Heath E., Macdonald R., Black S., 1996. U-series isotopes and destructive plate margin magma genesis in the Lesser Antilles. Earth Planet. Sci. Lett. 142, 191-207.

Turner, S., Handler, M., Bindeman, I., Suzuki, K., 2009. New insights into the origin of O-Hf-Os isotope signatures in arc lavas from Tonga-Kermadec. Chem. Geol., 266, 196-202.

van Gerven, M., Pichler, H., 1995. Some aspects of the volcanology and geochemistry of the Tengger Caldera, Java, Indonesia: eruption of a K-rich tholeiitic series. J. Southeast Asian Earth Sci. 11, 125-133.

Vervoort, J.D., Patchett, P.J., Blichert-Toft, J., Albarede, F., 1999. Relationships between Lu-Hf and Sm-Nd isotopic systems in the global sedimentary system. Earth Planet. Sci. Lett. 168, 79-99.

von Huene, R., Scholl. D.W., 1991. Observations at convergent margins concerning sediment subduction, subduction erosion, and the growth of continental crust. Rev. Geophys. 29, 279-316.

Vroon P.Z., 1992. Subduction of continental material in the Banda Arc, Eastern Indonesia: Sr-Nd-Pb isotope and trace-element evidence from volcanics and sediments. Ph.D. Thesis University of Utrecht.

Vroon, P.Z., van Bergen, M.J., Klaver, G. J., White, W.M., 1995. Strontium, neodymium, and lead isotopic and trace-element signatures of the East Indonesian sediments: Provenance and implications for Banda Arc magma genesis. Geochim. Cosmochim. Acta 59, 2573-2598.

Vukadinovic, D., Sutawidjaja, I., 1995. Geology, mineralogy and magma evolution of Gunung Slamet Volcano, Java, Indonesia. J. Southeast Asian Earth Sci. 11, 135-164.

Westbrook, G.K., Ladd, J.W., Buhl, P., Bangs, N., Tiley, G.J., 1988. Cross section of an accretionary wedge: Barbados Ridge Complex. Geology 16, 631-635.

White, W.M., Patchett, J., 1984. Hf-Nd-Sr isotopes and incompatible element abundances in island arcs: implications for magma origins and crustal-mantle evolution. Earth Planet. Sci. Lett. 67, 167-185.

White, W.M., Patchett, J., BenOthman, D., 1986. Hf isotope ratios of marine sediments and Mn nodules; evidence for a mantle source of Hf in seawater. Earth Planet. Sci. Lett. 79, 46-54.

Whitford, D.J., 1975. Geochemistry and petrology of volcanic rocks from the Sunda arc, Indonesia, PhD Thesis (unpublished), Australian National University, Canberra, Australia.

Whitford, D.J., Nicholls, I.A., 1976. Potassium variations in lavas across the Sunda arc in Java and Bali. In: R.W. Johnson (Editor), Volcanism in Australasia. Elsevier, Amsterdam, pp. 63-75.

Woodhead, J.D., Hergt, J.M., Davidson, J.P., Eggins, S.M., 2001. Hafnium isotope evidence for 'conservative' element mobility during subduction processes. Earth Planet. Sci. Lett. 192, 331-346.

Workman, R.K., Hart, S.R., 2005. Major and trace element composition of the depleted MORB mantle (DMM). Earth Planet. Sci. Lett. 231, 53-72.

You, C.-F., Castillo, P.R., Gieskes, J.M., Chan. L.H., Spivack, A.J., 1996. Trace element behaviour in hydrothermal experiments: Implications for fluid processes at shallow depths in subduction zones. Earth Planet. Sci. Lett. 140, 41-52.

Figure 1

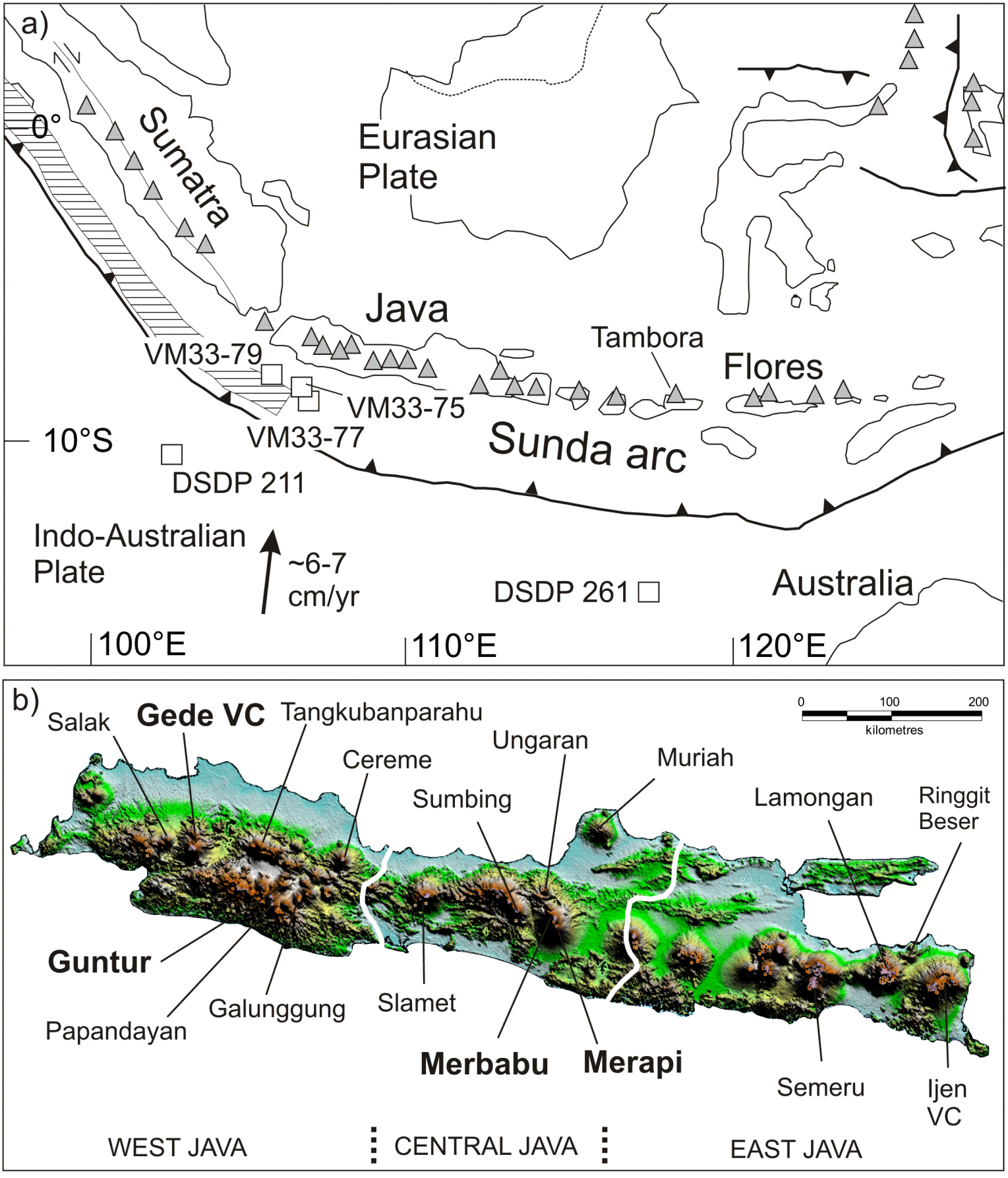
a)
0°
Sumatra
Eurasian
Plate
Java
Tambora
Flores
VM33-79
VM33-75
VM33-77
10°S
Sunda arc
DSDP 211
Indo-Australian
Plate
~6-7
cm/yr
DSDP 261
Australia
100°E
110°E
120°E
b)
0
100
200
kilometres
Salak
Gede VC
Tangkubanparahu
Ungaran
Cereme
Muriah
Sumbing
Lamongan
Ringgit
Beser
Guntur
Papandayan
Galunggung
Slamet
Merbabu
Merapi
Semeru
Ijen
VC
WEST JAVA
CENTRAL JAVA
EAST JAVA

Figure 2

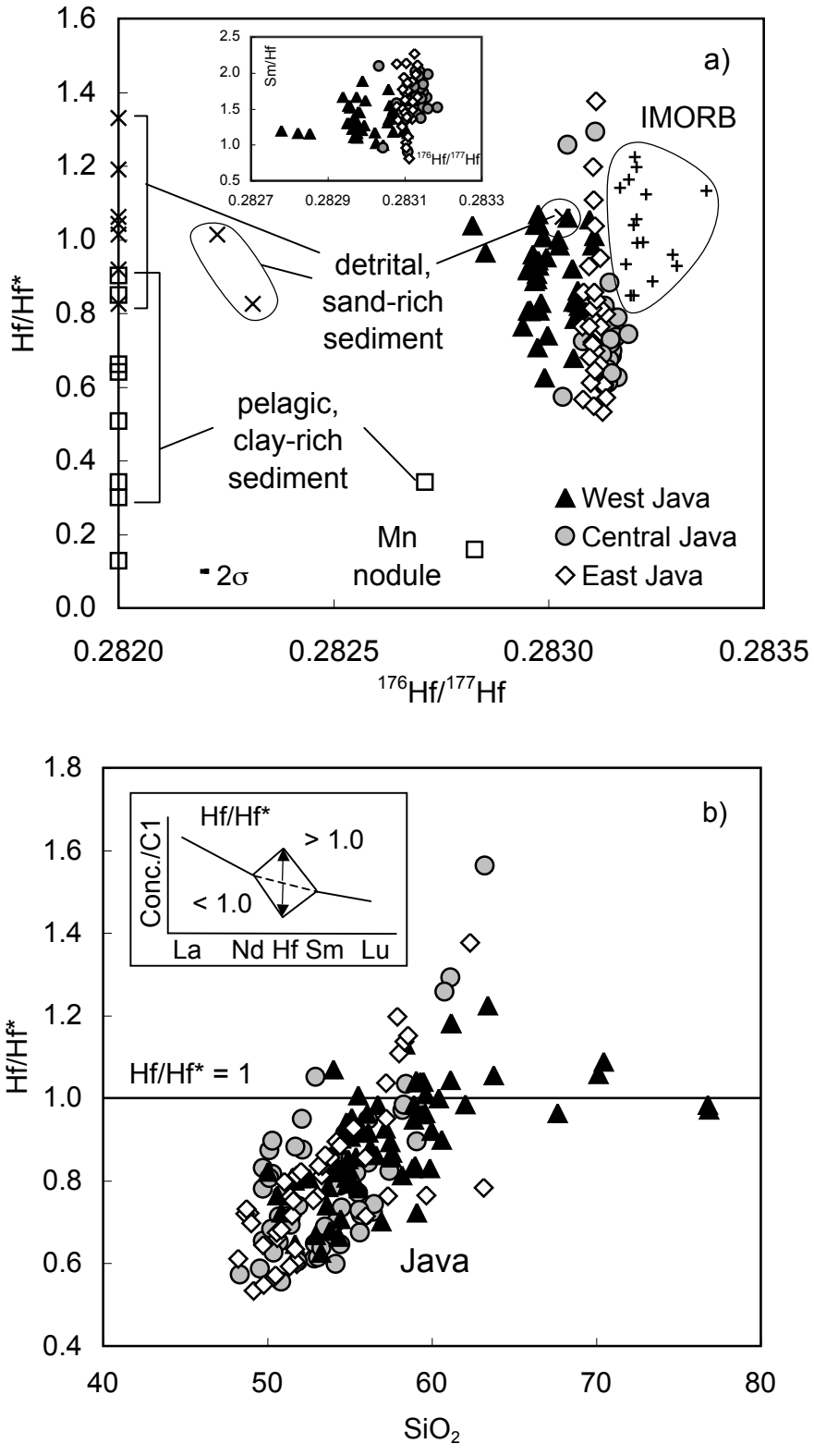
a)
IMORB
detrital,
sand-rich
sediment
pelagic,
clay-rich
sediment
Mn
nodule
2σ
West Java
Central Java
East Java
Hf/Hf*
176Hf/177Hf
Sm/Hf
b)
Hf/Hf* = 1
Java
SiO2
Conc./C1
> 1.0
< 1.0
La Nd Hf Sm Lu

Figure 3

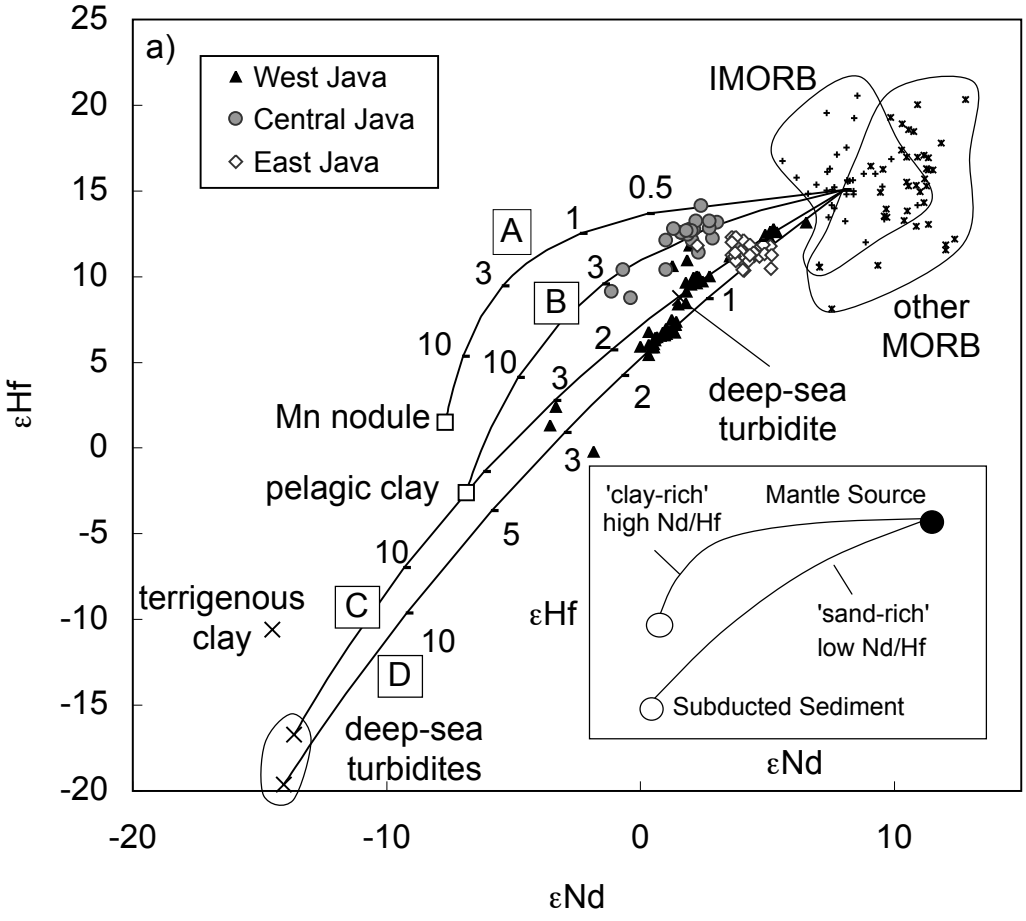
a)
West Java
Central Java
East Java
IMORB
other MORB
deep-sea turbidite
Mn nodule
pelagic clay
terrigenous clay
deep-sea turbidites
A
B
C
D
'clay-rich' high Nd/Hf
Mantle Source
'sand-rich' low Nd/Hf
Subducted Sediment
εHf
εNd

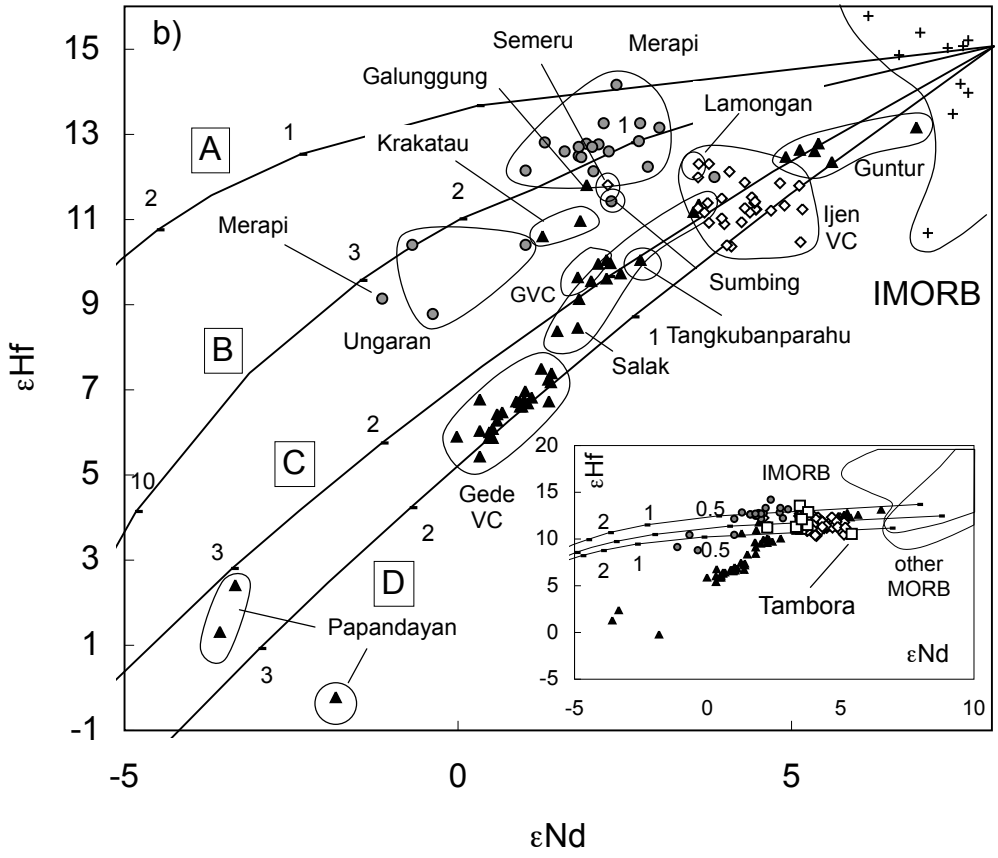
b)
Semeru
Merapi
Galunggung
Lamongan
Krakatau
Guntur
Merapi
Ijen VC
GVC
Sumbing
IMORB
Ungaran
1 Tangkubanparahu
Salak
Gede VC
Papandayan
Tambora
other MORB
A
B
C
D
εHf
εNd

Figure 4

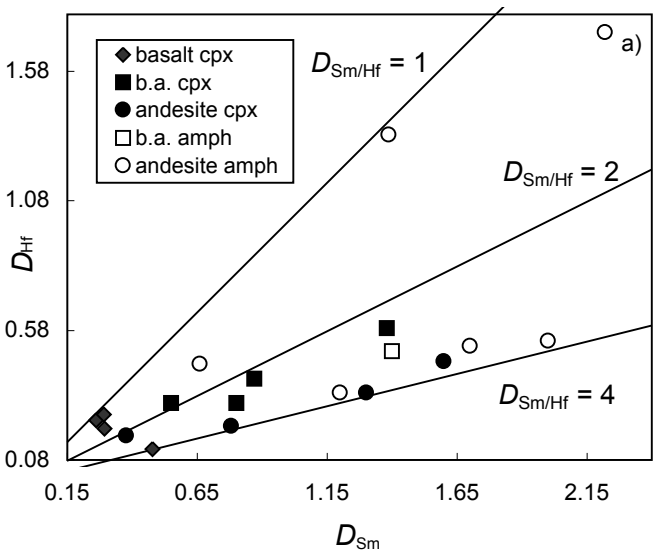
a)
basalt cpx
b.a. cpx
andesite cpx
b.a. amph
andesite amph
$D_{Sm/Hf}$ = 1
$D_{Sm/Hf}$ = 2
$D_{Sm/Hf}$ = 4
D_{Hf}
D_{Sm}
1.58
1.08
0.58
0.08
0.15
0.65
1.15
1.65
2.15

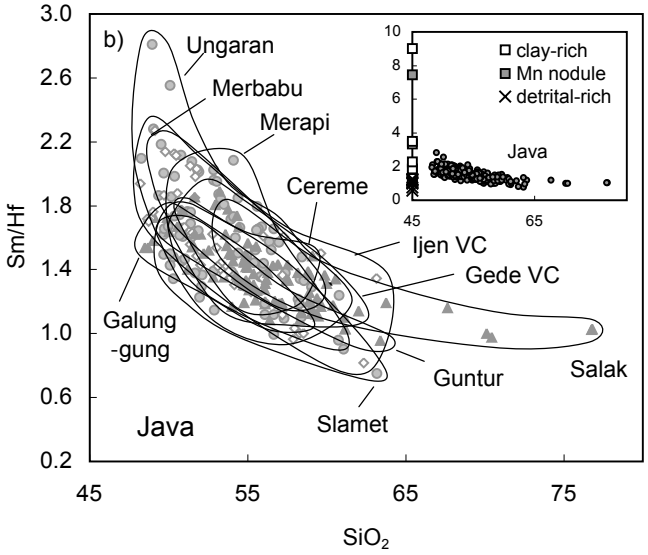
b)
Ungaran
Merbabu
Merapi
Cereme
Iljen VC
Gede VC
Galung
-gung
Guntur
Salak
Slamet
Java
clay-rich
Mn nodule
detrital-rich
Java
Sm/Hf
SiO_2
3.0
2.6
2.2
1.8
1.4
1.0
0.6
0.2
45
55
65
75

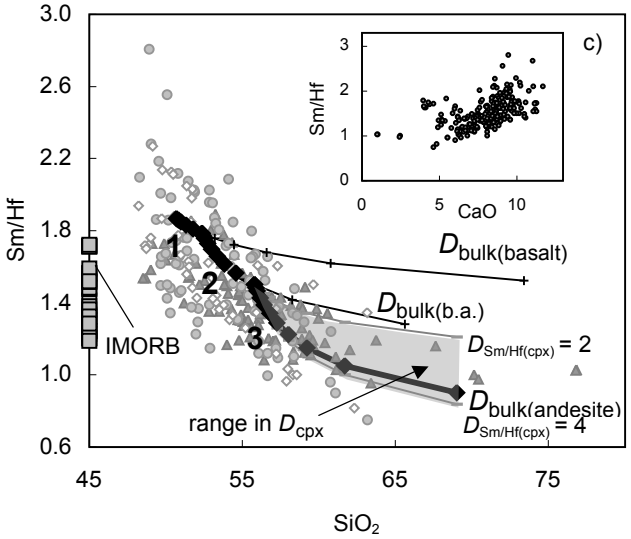
c)
IMORB
1
2
3
$D_{bulk(basalt)}$
$D_{bulk(b.a.)}$
$D_{Sm/Hf(cpx)}$ = 2
$D_{bulk(andesite)}$
$D_{Sm/Hf(cpx)}$ = 4
range in D_{cpx}
Sm/Hf
CaO
SiO_2
3.0
2.6
2.2
1.8
1.4
1.0
0.6
45
55
65
75

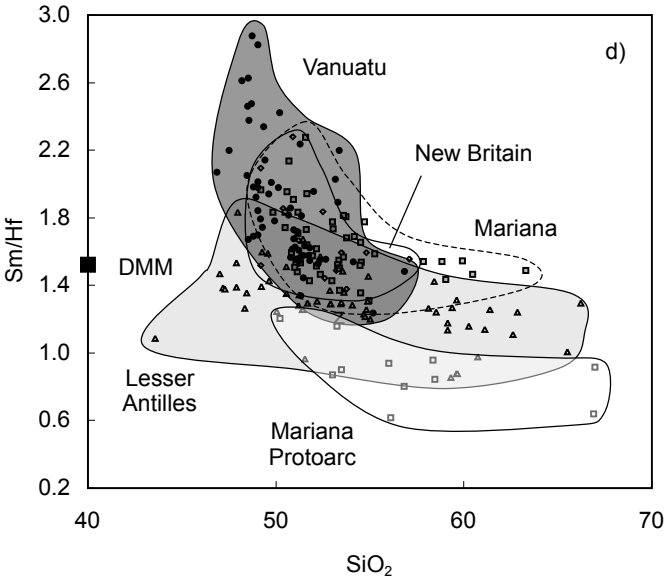
d)
Vanuatu
New Britain
Mariana
DMM
Lesser
Antilles
Mariana
Protoarc
Sm/Hf
SiO_2
3.0
2.6
2.2
1.8
1.4
1.0
0.6
0.2
40
50
60
70

Figure 5

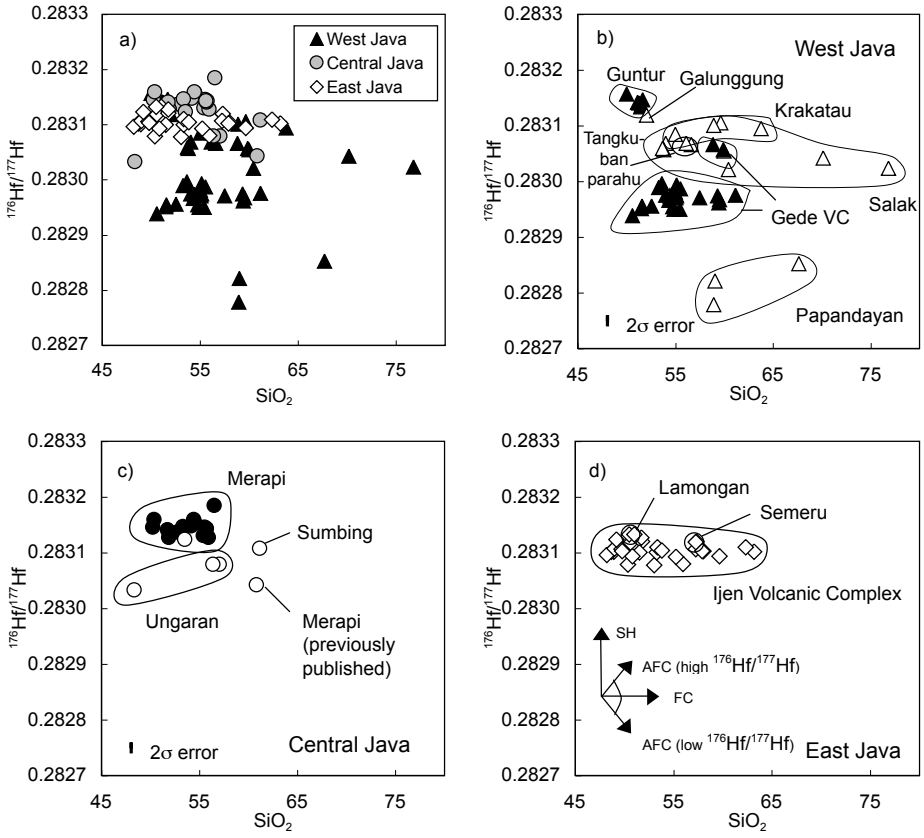
a)
West Java
Central Java
East Java
b)
West Java
Guntur
Galunggung
Krakatau
Tangku-
ban
parahu
Gede VC
Salak
Papandayan
2σ error
c)
Merapi
Sumbing
Ungaran
Merapi
(previously
published)
2σ error
Central Java
d)
Lamongan
Semeru
Ijen Volcanic Complex
SH
AFC (high 176Hf/177Hf)
FC
AFC (low 176Hf/177Hf)
East Java
176Hf/177Hf
SiO2
0.2833
0.2832
0.2831
0.2830
0.2829
0.2828
0.2827
45
55
65
75

Table 1. New Nd and Hf isotope data of volcanic rocks from Java

Province	Volcano	Sample	Latitude (S)	Longitude (E)	$^{143}Nd/^{144}Nd$	2σ	εNd	$^{176}Hf/^{177}Hf$	2σ	εHf
West Java	Gede VC	G01A	06°42'16.9"	107°01'39.6"	0.512647	15	0.33	0.282977	21	6.78
West Java	Gede VC	G01B	06°42'16.9"	107°01'39.6"	0.512653	10	0.46	0.282951	09	5.86
West Java	Gede VC	G10	06°44'51.5"	107°02'28.3"	0.512700	15	1.36	0.282975	07	6.72
West Java	Gede VC	G16	06°49'47.6"	106°55'35.3"	0.512629	12	-0.02	0.282952	10	5.90
West Java	Gede VC	G17	06°47'27.7"	106°59'40.6"	0.512681	16	0.99	0.282976	08	6.76
West Java	Gede VC	G18	06°47'23.5"	106°58'59.8"	0.512660	16	0.58	0.282963	08	6.28
West Java	Gede VC	G19	06°47'12.7"	106°58'43.1"	0.512701	11	1.39	0.282988	07	7.17
West Java	Gede VC	G20	06°47'03.1"	106°58'30.6"	0.512675	13	0.87	0.282975	08	6.73
West Java	Gede VC	G21	06°46'59.8"	106°58'44.8"	0.512678	21	0.93	0.282972	07	6.61
West Java	Gede VC	G22	Kawah Wadon crater edge		0.512664	14	0.66	0.282968	07	6.46
West Java	Gede VC	G23	06°46'40.5"	106°58'31.7"	0.512656	12	0.52	0.282957	08	6.07
West Java	Gede VC	G25	06°46'03.0"	106°58'49.1"	0.512677	15	0.92	0.282975	09	6.71
West Java	Gede VC	G26	50m from the Gede Observatory		0.512694	16	1.24	0.282997	07	7.49
West Java	Gede VC	G28	06°43'05.6"	106°57'54.4"	0.512683	11	1.04	0.282974	15	6.68
West Java	Gede VC	G30	06°42'36.5"	106°56'47.2"	0.512646	12	0.32	0.282956	08	6.04
West Java	Gede VC	G33	06°42'20.4"	106°58'35.8"	0.512699	09	1.35	0.282990	10	7.24
West Java	Gede VC	G35	06°49'48.6"	106°55'58.7"	0.512646	12	0.32	0.282939	09	5.44
West Java	Gede VC	G36A	06°49'48.6"	106°55'58.7"	0.512654	11	0.47	0.282955	11	6.01
West Java	Gede VC	G40	06°44'20.9"	107°00'30.6"	0.512679	10	0.96	0.282972	08	6.61
West Java	Gede VC	G42	06°44 51.5"	107°00'20.6"	0.512660	14	0.58	0.282967	08	6.43
West Java	Gede VC	G44	06°45'19.1"	107°01'04.4"	0.512702	14	1.40	0.282994	11	7.38
West Java	Gede VC	G46	06°47'42.6"	107°01'09.1"	0.512682	13	1.01	0.282982	14	6.96
West Java	Gede VC	G49	06°46'41.2"	107°03'50.7"	0.512722	10	1.79	0.283058	09	9.65
West Java	Gede VC	G51	06°42'16.9"	107°01'39.6"	0.512656	11	0.52	0.282951	08	5.86
West Java	Gede VC	G52	06°44'32.7"	107°03'55.3"	0.512737	11	2.10	0.283067	07	9.96
West Java	Gede VC	G55	06°48'46.7"	107°03'28.0"	0.512687	20	1.11	0.282978	07	6.82
West Java	Guntur	GU1/T	07°10'30"	107°51'06"	0.512982	08	6.87	0.283157	10	13.16
West Java	Guntur	GU5/T	07°10'18"	107°52'00"	0.512907	16	5.40	0.283147	07	12.79
West Java	Guntur	GU7/T	07°10'42"	107°51'48"	0.512917	10	5.60	0.283134	09	12.35
West Java	Guntur	GU9/T	07°10'30"	107°52'12"	0.512904	08	5.34	0.283142	13	12.61
West Java	Guntur	GU15/T	07°09'48"	107°52'30"	0.512882	15	4.91	0.283137	09	12.46
West Java	Guntur	GU16/T	07°09'54"	107°52'42"	0.512893	15	5.12	0.283142	09	12.63
Central Java	Merapi*	M95-026	07°31'46"	110°28'42"	0.512738[a]	*09*	2.11	0.283146	10	12.76
Central Java	Merapi*	M95-028	07°35'08"	110°25'37"	0.512729	10	1.93	0.283146	14	12.77
Central Java	Merapi*	M96-050	07°35'11"	110°25'36"	0.512742	08	2.18	0.283160	09	13.25
Central Java	Merapi	M96-056	07°33'37"	110°27'38"	0.512776[a]	*10*	2.85	0.283131	10	12.23
Central Java	Merapi	M96-073	07°34'30"	110°23'13"	0.512785[a]	*09*	3.02	0.283157	16	13.15
Central Java	Merapi	M96-137	07°33'28"	110°24'01"	0.512769[a]	*07*	2.71	0.283148	11	12.83
Central Java	Merapi*	M96-142	07°25'36"	110°34'50"	0.512734[a]	*10*	2.03	0.283128	11	12.13
Central Java	Merapi*	M96-175	07°31'38"	110°28'12"	0.512752	12	2.38	0.283185	16	14.15
Central Java	Merapi	M97-021	07°35'24"	110°25'23"	0.512723[a]	*09*	1.81	0.283138	10	12.48
Central Java	Merapi	M97-031	07°36'05"	110°25'11"	0.512712[a]	*10*	1.60	0.283141	09	12.58
Central Java	Merapi	M97-0392	07°30'44"	110°25'23"	0.512725[a]	*11*	1.85	0.283137	11	12.45
Central Java	Merapi	M97-068	07°34'06"	110°22'51"	0.512682[a]	*09*	1.01	0.283128	12	12.13
Central Java	Merapi	M98-031	07°31'03"	110°20'48"	0.512746[a]	*09*	2.26	0.283141	11	12.58
Central Java	Merapi	M98-047	07°32'29"	110°29'07"	0.512723[a]	*09*	1.81	0.283144	07	12.69
Central Java	Merapi	M98-0532	07°30'59"	110°31'21"	0.512770[a]	*10*	2.73	0.283160	12	13.25
Central Java	Merapi	M98-096	07°29'57"	110°24'36"	0.512697[a]	*10*	1.31	0.283147	13	12.80
Central Java	Merapi*	M98-107	07°32'19"	110°27'26"	0.512733[a]	*10*	2.01	0.283144	10	12.69

All new data are presented relative to a JMC 475 $^{176}Hf/^{177}Hf$ value of 0.282160 (Nowell et al., 1998) and a J&M $^{143}Nd/^{144}Nd$ value of 5.11110 (Royse et al., 1998), corresponding to Ames $^{143}Nd/^{144}Nd$ of 0.512130 and La Jolla $^{143}Nd/^{144}Nd$ of 0.51186.

εHf and εNd values were calculated relative to CHUR values of 0.282785 for $^{176}Hf/^{177}Hf$ and 0.512630 for $^{143}Nd/^{144}Nd$ (Bouvier et al., 2008).

[a]Gertisser and Keller (2003) $^{143}Nd/^{144}Nd$ data are presented relative to an Ames $^{143}Nd/^{144}Nd$ of 0.512130.

Errors in italic are within-run 2SE on the final quoted significant figure taken from Gertisser and Keller (2003).

Location information for Gede VC and Guntur samples are taken from Handley (2006) and Edwards (1990), respectively.

For sample location information and unit descriptions of Merapi volcanic rocks, see Gertisser (2001).

* indicates sample locations recalculated with GPS software from UTM co-ordinates.

Table 2. New major element, trace element and Sr-Nd isotope data of Merbabu and Merapi (Central Java) volcanic rocks

Volcano	Merbabu	Merbabu	Merbabu	Merbabu	Merbabu	Merbabu	Merapi	Merapi	Merapi	Merapi*	Merapi*	Merapi*
Latitude (S)	07°29'53"	07°30'00"	07°31'08"	07°23'54"	07°21'52"	07°29'13"	07°35'18"	07°32'19"	07°31'03"	07°35'08"	07°35'11"	07°31'38"
Longitude (E)	110°25'46"	110°25'11"	110°21'37"	110°25'53"	110°27'44"	110°34'06"	110°26'34"	110°23'16"	110°20'48"	110°25'37"	110°25'36"	110°28'12"
Sample	MB-1	MB-2	MB-6	MB-16	MB-22	MB-28	M96-102	M98-030	M98-031	M95-028	M96-050	M96-175
SiO_2	49.55	49.70	50.81	59.07	58.28	51.41	*51.87*	*52.13*	*51.70*	50.20	50.37	56.49
Al_2O_3	21.22	17.23	19.73	18.87	18.76	17.64	*20.44*	*19.02*	*18.77*	19.78	18.68	18.71
Fe_2O_3	9.44	11.01	9.95	6.64	7.14	10.19	*8.24*	*8.49*	*8.38*	9.53	10.12	7.45
MgO	3.18	5.75	3.78	1.95	2.27	4.54	*2.47*	*2.80*	*3.09*	3.19	4.28	2.58
CaO	10.21	10.81	8.57	6.08	6.72	9.26	*8.86*	*8.72*	*9.23*	9.72	9.26	8.09
Na_2O	2.84	2.76	2.78	3.52	3.51	3.09	*3.35*	*3.39*	*3.35*	3.19	3.18	3.59
K_2O	1.76	1.47	2.24	1.91	1.74	2.10	*1.74*	*1.99*	*1.90*	1.97	1.83	1.59
TiO_2	0.86	0.83	0.81	0.70	0.73	1.03	*0.81*	*0.78*	*0.84*	1.03	1.09	0.72
MnO	0.17	0.21	0.18	0.17	0.18	0.17	*0.20*	*0.20*	*0.20*	0.13	0.14	0.17
P_2O_5	0.26	0.18	0.32	0.31	0.30	0.31	*0.31*	*0.31*	*0.26*	0.28	0.28	0.29
LOI	0.66	0.04	1.12	0.71	0.44	-0.44	*1.63*	*2.07*	*2.49*	1.14	1.40	0.71
Total	100.15	99.99	100.29	99.93	100.07	99.30	*99.92*	*99.90*	*100.21*	100.16	100.62	100.40
V	249	333	256	92	113	295	259	152	169	331	298	151
Cr	26.0	69.0	14.8	5.7	7.3	59.9	6.0	2.4	2.5	124.1	34.3	10.4
Co	23.0	33.8	25.2	7.5	9.2	30.0	22.9	11.3	13.0	31.0	28.1	14.6
Ni	8.9	19.8	8.9	< d.l.	< d.l.	15.3	7.0	2.2	2.1	43.1	16.4	< d.l.
Cu	148	143	216	19	16	151	36	13	13	n.m.	n.m.	n.m.
Zn	84	89	89	95	91	101	76	76	75	n.m.	n.m.	n.m.
Ga	21	17	19	20	21	21	19	21	21	n.m.	n.m.	n.m.
Rb	24.8	29.4	53.6	45.0	38.5	44.2	24.6	20.5	20.7	23.9	36.2	37.8
Sr	592	460	565	437	431	421	533	544	531	568	467	529
Y	18.2	17.2	19.4	25.5	23.3	23.3	25.0	26.9	24.7	18.0	21.1	22.4
Zr	62	49	65	156	139	85	104	144	133	64	68	114
Nb	1.94	1.50	2.18	6.65	5.73	3.11	4.35	6.28	5.63	2.02	2.42	4.49
Cs	0.78	2.43	3.34	4.87	3.25	3.72	2.04	1.81	1.83	n.m.	n.m.	n.m.
Ba	546	462	677	487	431	545	364	291	307	474	584	428
La	14.6	11.0	19.4	24.1	21.2	17.5	16.3	16.9	14.8	11.6	14.3	18.9
Ce	29.3	21.5	36.5	48.6	42.6	35.0	33.4	37.0	33.8	23.3	28.7	38.2
Pr	3.44	2.72	4.24	5.82	5.30	4.34	4.552	5.288	4.736	2.84	3.57	4.78
Nd	14.9	11.7	18.3	23.2	20.4	18.0	20.0	23.4	21.0	12.1	15.5	20.0
Sm	3.91	3.18	4.12	5.06	4.52	4.17	4.72	5.39	4.97	3.10	3.82	4.22
Eu	1.23	1.06	1.38	1.55	1.43	1.33	1.40	1.53	1.45	1.10	1.33	1.43
Gd	3.60	3.26	4.09	4.70	4.41	4.24	4.74	5.13	4.77	3.15	3.91	4.13
Tb	0.534	0.447	0.610	0.756	0.656	0.629	0.759	0.832	0.773	0.473	0.557	0.603
Dy	3.26	2.87	3.45	4.31	4.14	3.88	4.48	4.82	4.49	2.88	3.49	3.77
Ho	0.601	0.623	0.683	0.859	0.849	0.856	0.926	1.006	0.932	0.606	0.723	0.739
Er	1.73	1.76	2.01	2.59	2.37	2.22	2.52	2.73	2.49	1.69	1.99	2.31
Tm	0.29	0.27	0.33	0.42	0.41	0.40	0.391	0.428	0.395	0.258	0.297	0.326
Yb	1.72	1.78	2.00	2.80	2.47	2.23	2.54	2.84	2.59	1.61	1.98	2.11
Lu	0.280	0.287	0.325	0.470	0.434	0.377	0.416	0.467	0.431	0.249	0.331	0.366
Hf	1.79	1.59	1.95	3.92	3.82	2.47	2.88	3.95	3.62	1.67	1.93	2.77
Ta	0.16	0.13	0.19	0.56	0.50	0.25	0.31	0.47	0.41	0.15	0.20	0.38
Pb	21.6	16.3	25.3	21.2	18.6	22.8	14.9	21.3	20.0	16.6	18.3	25.4
Th	6.43	4.37	8.74	9.27	7.98	7.75	5.27	8.18	7.14	4.91	5.46	5.68
U	0.82	0.99	1.79	1.95	1.76	1.71	1.06	1.11	1.09	0.84	1.08	1.35
$^{87}Sr/^{86}Sr$	0.705888	0.705768	0.705825	0.705672	0.705686	0.705812	*0.705515*	*0.705704*	*0.705540*	0.705793	0.705539	0.705105
2SE	10	10	10	10	09	10	*09*	*10*	*09*	09	09	10
$^{143}Nd/^{144}Nd$	0.512663	0.512699	0.512653	0.512707	0.512701	0.512683	*0.512753*	*0.512732*	*0.512746*	0.512729	0.512742	0.512752
2SE	08	08	08	07	12	09	*09*	*06*	*09*	10	08	12

Major element and Sr-Nd isotope data of Gertisser and Keller (2003) shown by italic font.
< d.l., below detection limit (<5 ppm for Ni); n.m., not measured.
$^{87}Sr/^{86}Sr$ isotope data presented relative to a NBS 987 $^{87}Sr/^{86}Sr$ value of 0.710240.
$^{143}Nd/^{144}Nd$ isotope data presented relative to an Ames $^{143}Nd/^{144}Nd$ value of 0.512130.
Errors on isotope data are within-run 2SE on the final quoted significant figure.

Table 3. End member compositions used in Hf-Nd isotope mixing calculations

	Nd (ppm)	Hf (ppm)	$^{143}Nd/^{144}Nd$	$^{176}Hf/^{177}Hf$
IMORB Source	0.97	0.25	0.513042	0.283211
Sed A	187.9	5.73	0.512236	0.282828
Sed B	55.3	3.67	0.512278	0.282712
Sed C	35	5.09	0.511930	0.282311
Sed D	31.3	5.58	0.511910	0.282230

Mantle wedge represented by I-MORB source (I-MORB/10 assuming 10% melting) IMORB data from Chauvel and Blichert-Toft (2001). IMORB average Nd and Hf concentration, Nd and Hf isotope data from Chauvel and Blichert-Toft, 2001.
Local sediments: A = Mn nodule (V34-62, Ben Othman et al., 1989; White et al., 1986) B = pelagic clay (V34-45 White et al., 1986; Ben Othman et al., 1989); C and D = deep sea turbidite sediments V28-357-M (CA30-M) and V28-357-M (CA30-S), respectively (Vervoort et al., 1999).

Appendix B. Additional analytical information

Table B.1. Accepted element abundances of international rock standards compared to those measured over the period of study. Detection limits and maximum measured blanks.

	BIR1			W2			BHVO-1			AGV1		
	Accepted	This study		Accepted	This study		Accepted	This study		Accepted	This study	
PPM	value	value (n = 26)	1SD	value	value (n = 13)	1SD	value	value (n = 23)	1SD	value	value (n = 12)	1SD
Sc	44	43	4.70	35	36	1	31.8	31	2	12.1	12	1
Ti (wt%)	0.96	0.97	0.08	1.06	1.07	0.07	2.71	2.79	0.12	1.06	1.03	0.06
V	313	334	16.60	262	272	8	317	319	10	123	121	4
Cr	382	418.4	25.2	93	92.5	3.4	289	295.1	8.5	12	7.0	3.4
Mn (wt%)	0.171	0.18	0.01	0.163	0.17	0.01	0.168	0.17	0.01	0.096	0.10	0.01
Co	51.4	55	2	44	45	1	45	45	1	15.1	16	0
Ni	166	199.8	8.2	70	81.4	2.1	121	134.7	3.4	17	16.7	0.7
Cu	126	120	5	103	104	3	136	138	3	60	58	2
Zn	71	69	8	77	84	27	105	108	5	88	84	3
Ga	16	15	1	20	18	0	21	21	1	20	20	0
Rb	0.27	0.2	0.0	20	20.2	0.4	11	9.5	0.2	67	67.2	1.2
Sr	108	110	12	194	201	9	403	391	22	662	676	32
Y	16	16	1	24	23	0	27.6	28	0	21	20	0
Zr	22	15	0	94	91	2	179	175	2	225	229	3
Nb	2	0.57	0.02	7.9	7.66	0.09	19	19.39	0.18	15	14.52	0.14
Cs	0.45	0.00	0.02	0.99	0.89	0.04	0.13	0.10	0.03	1.26	1.24	0.04
Ba	7.7	7	0	182	177	4	139	138	3	1221	1219	25
La	0.88	0.6	0.0	11.4	10.8	0.2	15.8	15.6	0.3	38	37.9	0.7
Ce	2.5	1.9	0.0	24	23.4	0.4	39	37.8	0.6	66	66.8	1.2
Pr	0.5	0.38	0.01	5.9	3.18	0.04	5.7	5.62	0.09	6.5	8.65	0.19
Nd	2.5	2.5	0.1	14	13.9	0.2	25.2	26.3	0.4	34	33.2	0.6
Sm	1.08	1.11	0.04	3.25	3.38	0.04	6.2	6.31	0.10	5.9	5.85	0.12
Eu	0.54	0.51	0.02	1.1	1.11	0.01	2.06	2.07	0.03	1.66	1.68	0.03
Gd	1.9	1.94	0.04	3.6	3.86	0.06	6.4	6.55	0.13	5.2	4.83	0.10
Tb	0.41	0.38	0.01	0.63	0.65	0.01	0.96	0.98	0.01	0.71	0.67	0.01
Dy	2.4	2.54	0.08	3.8	3.87	0.06	5.2	5.33	0.07	3.8	3.53	0.06
Ho	0.5	0.57	0.02	0.76	0.80	0.01	0.99	1.00	0.01	0.73	0.67	0.01
Er	1.8	1.62	0.06	2.5	2.15	0.02	2.4	2.43	0.02	1.61	1.73	0.03
Tm	0.27	0.27	0.01	0.38	0.34	0.01	0.33	0.35	0.01	0.32	0.27	0.01
Yb	1.7	1.64	0.07	2.05	2.07	0.02	2.02	2.01	0.02	1.67	1.65	0.03
Lu	0.26	0.27	0.01	0.33	0.33	0.00	0.291	0.30	0.00	0.28	0.27	0.01
Hf	0.58	0.59	0.02	2.56	2.42	0.04	4.38	4.47	0.04	5.1	5.12	0.09
Ta	0.062	0.05	0.01	0.5	0.50	0.01	1.23	1.26	0.01	0.92	0.91	0.01
tot Pb	3.2	3.2	0.3	9.3	7.9	0.2	2.6	2.2	0.1	36	35.7	0.7
Th	0.031	0.03	0.00	2.2	2.21	0.07	1.08	1.26	0.03	6.5	6.34	0.20
U	0.01	0.01	0.00	0.53	0.49	0.01	0.42	0.42	0.01	1.89	1.87	0.06

	BE-N			NBS688			detection	detection	maximum blank
	Accepted	This study		Accepted	This study		limit	limit	measured
PPM	value	value (n = 11)	1SD	value	value (n = 14)	1SD	solid ng g^{-1}	soln pg ml^{-1}	(n = 70, ppm)
Sc	22	23	1	38	38	2	212	42	1
Ti (wt%)	2.61	2.66	0.13	1.17	1.16	0.07	6380	1280	0.00
V	235	233	9	242	252	8	273	55	0
Cr	360	368.1	15.6	332	333.1	11.7	532	106	1.6
Mn (wt%)	0.2	0	0	0.167	0	0	231	46	0
Co	61	62	2	49	49	2	19.5	3.9	0
Ni	267	300.9	10.4	158	173.4	5.5	897	179	0.6
Cu	72	72	3	96	87	3	128	26	0
Zn	120	121	4	84	79	13			65
Ga	17	18	1	17	16	0	34.3	6.9	0
Rb	47	48.2	1.5	1.91	2.0	0.1	13.4	2.7	0.0
Sr	1370	1538	138	169.2	174	7	43	0.64	0
Y	30	31	1	17	21	0	20.9	4.2	0
Zr	265	273	5	61	56	1	25.2	5	3
Nb	100	117.56	1.49	5	4.33	0.06	9.72	1.9	0.02
Cs	0.8	0.75	0.04	0.24	0.02	0.04	3.79	0.8	0.05
Ba	1025	1059	24	200	178	4	111	22	3
La	82	82.1	1.6	5.3	5.3	0.1	3.73	0.75	0.0
Ce	152	147.9	2.2	13	12.0	0.2	12.2	2.4	0.0
Pr	16.9	17.96	0.35	2.4	1.82	0.03	2.57	0.51	0.03
Nd	70	69.9	1.1	9.6	8.9	0.1	13.2	2.6	0.0
Sm	12	12.42	0.21	2.5	2.44	0.03	2.84	0.57	0.05
Eu	3.6	3.72	0.04	1.01	0.99	0.01	1.78	0.36	0.01
Gd	9	10.18	0.19	3.2	3.12	0.08	3.01	0.6	0.03
Tb	1.3	1.33	0.02	0.52	0.54	0.01	0.3	0.06	0.01
Dy	6.29	6.41	0.08	3.4	3.42	0.05	2.12	0.42	0.04
Ho	1.03	1.09	0.01	0.81	0.74	0.01	0.4	0.08	0.01
Er	2.48	2.44	0.04	2.1	2.07	0.03	0.23	0.05	0.01
Tm	0.37	0.33	0.02	0.29	0.33	0.01	0.4	0.08	0.00
Yb	1.8	1.85	0.03	2.05	2.09	0.03	0.44	0.09	0.01
Lu	0.24	0.27	0.00	0.35	0.35	0.01	0.12	0.02	0.01
Hf	5.4	5.79	0.09	1.55	1.53	0.03	4.46	0.89	0.07
Ta	5.5	6.15	0.06	0.31	0.30	0.01	0.68	0.14	0.01
tot Pb	4	4.1	0.1	3.3	3.3	0.6	25.4	5.1	2.1
Th	11	10.72	0.28	0.33	0.35	0.02	2.73	0.55	0.01
U	2.4	2.43	0.07	0.31	0.29	0.03	0.78	0.16	0.00

Accepted standard values taken from Potts et al., 1992

Table B.2. Comparison of trace element concentrations of the internal standard (KI 202) analysed over the period of study

PPM	KI 202	KI 202	KI 202	KI 202	KI 202	KI 202	KI 202	KI 202	KI 202	AVERAGE	1SD	2SD	RSD
Sc	17	18	17	17	17	17	18	16	16	17	0.6	1.3	3.8
Ti (wt%)	0.75	0.85	0.82	0.81	0.82	0.82	0.82	0.72	0.76	0.80	0.0	0.1	5.3
V	179	182	179	173	176	176	177	179	166	176	4.6	9.3	2.6
Cr	2.6	2.2	1.2	2.8	2.8	2.8	2.8	2.4	1.8	2.4	0.6	1.1	23.7
Mn (wt%)	0.15	0.16	0.16	0.15	0.16	0.16	0.16	0.15	0.15	0.15	0.0	0.0	2.3
Co	37	39	39	38	38	38	38	38	36	38	1.0	2.1	2.7
Ni	4.7	4.7	4.0	4.0	3.6	3.7	3.7	4.8	4.1	4.2	0.5	1.0	11.4
Cu	38	40	38	39	39	39	40	39	36	39	1.3	2.6	3.4
Zn	62	67	67	68	70	68	71	66	63	67	2.9	5.9	4.4
Ga	17	18	18	17	17	17	17	17	17	17	0.5	1.0	2.9
Rb	62.8	72.6	72.1	71.0	70.7	70.9	71.5	71.3	66.2	69.9	3.2	6.5	4.6
Sr	342	427	429	412	411	412	412	381	387	401	27.5	55.0	6.9
Y	26	28	28	28	28	28	28	28	26	27	0.9	1.9	3.4
Zr	168	180	181	178	177	177	177	179	165	176	5.6	11.1	3.2
Nb	7.90	8.41	8.55	8.38	8.34	8.34	8.40	8.36	7.84	8.28	0.2	0.5	2.9
Cs	2.9	3.1	3.1	3.1	3.0	3.0	3.0	3.0	2.8	3.0	0.1	0.2	3.1
Ba	484	628	646	646	643	640	641	655	602	621	53.4	106.9	8.6
La	19.4	20.6	21.1	21.1	21.0	20.8	20.9	21.5	19.7	20.7	0.7	1.4	3.4
Ce	39.9	41.3	42.0	42.0	42.2	42.0	42.1	43.2	39.5	41.6	1.2	2.3	2.8
Pr	5.20	5.36	5.40	5.37	5.43	5.30	5.36	5.52	5.06	5.33	0.1	0.3	2.5
Nd	21.2	22.1	22.2	22.2	22.5	22.2	22.4	22.8	20.9	22.1	0.6	1.2	2.8
Sm	4.57	4.74	4.81	4.79	4.82	4.79	4.85	4.93	4.53	4.76	0.1	0.3	2.7
Eu	1.14	1.23	1.24	1.20	1.22	1.21	1.23	1.26	1.14	1.21	0.0	0.1	3.5
Gd	4.44	4.79	4.75	4.75	4.74	4.73	4.86	4.86	4.46	4.71	0.2	0.3	3.2
Tb	0.70	0.76	0.74	0.75	0.76	0.76	0.75	0.76	0.71	0.74	0.0	0.0	3.3
Dy	4.12	4.41	4.39	4.40	4.43	4.40	4.40	4.50	4.18	4.36	0.1	0.2	2.8
Ho	0.86	0.92	0.94	0.92	0.92	0.92	0.92	0.93	0.88	0.91	0.0	0.1	2.9
Er	2.42	2.53	2.62	2.59	2.60	2.54	2.57	2.59	2.41	2.54	0.1	0.2	3.1
Tm	0.42	0.43	0.44	0.41	0.41	0.40	0.42	0.42	0.38	0.41	0.0	0.0	3.9
Yb	2.55	2.72	2.73	2.70	2.71	2.71	2.70	2.72	2.56	2.68	0.1	0.1	2.7
Lu	0.42	0.46	0.46	0.45	0.45	0.45	0.45	0.45	0.43	0.45	0.0	0.0	3.0
Hf	4.41	4.65	4.73	4.63	4.63	4.62	4.69	4.71	4.42	4.61	0.1	0.2	2.5
Ta	0.77	0.81	0.81	0.81	0.82	0.81	0.82	0.81	0.77	0.80	0.0	0.0	2.4
tot Pb	10.4	11.5	11.6	11.6	11.6	11.6	11.6	11.7	10.5	11.3	0.5	1.0	4.6
Th	7.33	8.00	8.25	8.24	8.27	8.14	8.20	8.29	7.46	8.02	0.4	0.7	4.6
U	1.78	1.93	1.99	1.968	2.01	1.962	1.983	2.02	1.79	1.94	0.1	0.2	4.7

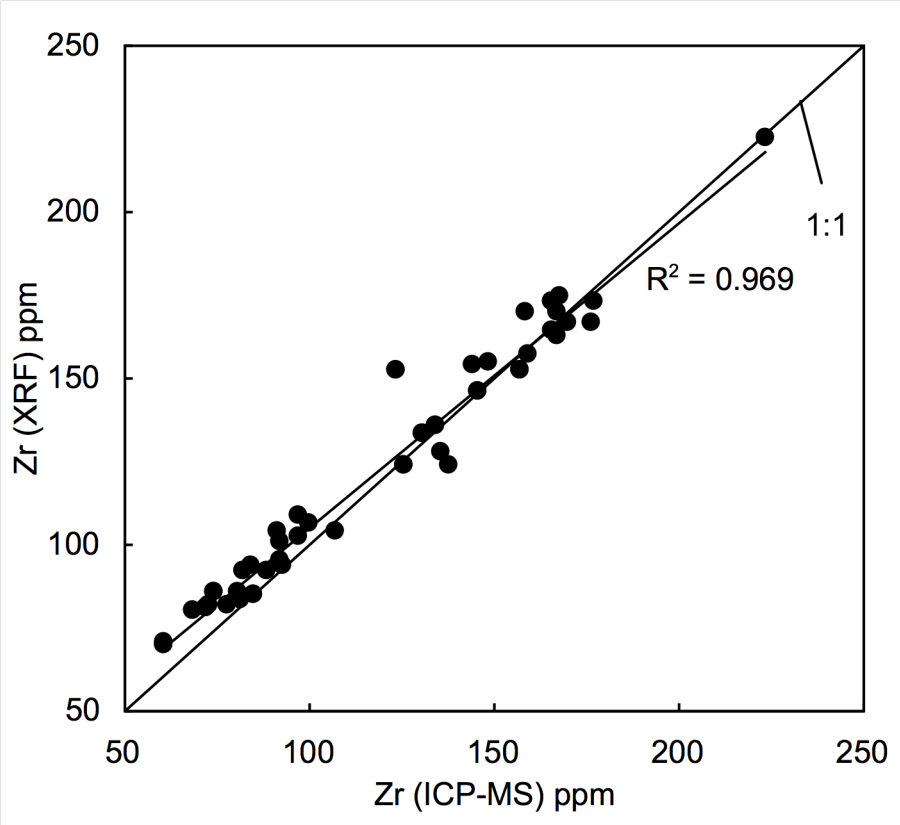

Fig. B.1. Comparison of ICP-MS (Handley et al., 2007) versus XRF (Sitorus, 1990) Zr concentration data for IVC volcanic rocks.

Table B.3. Average reproducibility and accuracy of Nd and Hf isotope ratios for standard solutions measured during this study

Element and Standard	Ratio	Accepted or reported value	# standards run	Mean measured value	Error (± 2SD absolute)	Error (± 2SD ppm)
Nd (J&M - pure)	143Nd/144Nd	0.511110[a]	44	0.511106	0.000009	18
Nd (J&M - Sm doped)	143Nd/144Nd	0.511110[a]	30	0.511108	0.000009	17
Nd (J&M all)	143Nd/144Nd	0.511110[a]	74	0.511106	0.000010	19
Hf (JMC 475 - H-CONE)	176Hf/177Hf	0.282160[b]	11	0.282160	0.000008	28
Hf (JMC 475 - ARIDUS X-CONE)	176Hf/177Hf	0.282160[b]	51	0.282146	0.000004	15

References: a Royse et al., 1998; b Nowell et al., 1998.
Aridus and X-cone long-term average up to period of study at Durham = 0.282145, 2RSD=26 ppm, n = 79 (Nowell et al., 2003; Pearson and Nowell, 2005).

Table B.4. Inter-laboratory comparison of Guntur $^{143}Nd/^{144}Nd$ isotope data

Sample	$^{143}Nd/^{144}Nd$ Edwards et al., 1993	$^{143}Nd/^{144}Nd$ This study	2σ error This study	difference (outside of known error)
GU1/T	0.512964[a]	0.512982[c]	0.000008	0.000010
GU5/T	0.512899[a]	0.512907[c]	0.000016	within error
GU7/T	0.512905[b]	0.512917[c]	0.000010	0.000002
GU9/T	0.512920[b]	0.512904[c]	0.000008	0.000008

Edwards et al. (1993) data are presented relative to La Jolla $^{143}Nd/^{144}Nd$ of 0.51186.
Measured at: a, Department of Terrestrial magnetism Carnegie Institute of Washington;
b, Royal Holloway College University of London; c, Arthur Holmes Isotope Geology Laboratory at Durham University.
Guntur sample repeats in this study presented relative to J&M $^{143}Nd/^{144}Nd$ of 0.511110.
$^{143}Nd/^{144}Nd$ error information is not given in Edwards et al., 1993.

References:

Edwards, CMH, Morris, JD, Thirlwall, MF, 1993. Separating mantle from slab signatures in arc lavas using B/Be and radiogenic isotope systematics. Nature, 362: 530-533.

Handley HK, Macpherson CG, Davidson JP, Berlo K, Lowry D, 2007. Constraining fluid and sediment contributions to subduction-related magmatism in Indonesia: Ijen Volcanic Complex, Indonesia. J Petrol 48:1155-1183.

Nowell, GM, Kempton, PD, Noble, SR, Fitton, JG, Saunders, AD, Mahoney, JJ, Taylor, RN, 1998. High precision Hf isotope measurements of MORB and OIB by thermal ionisation mass spectrometry: insights into the depleted mantle. Chemical Geology, 149: 211-233.

Nowell, GM, Pearson, DG, Ottley, CJ, Schweiters, J, 2003. Long-term performance characteristics of a plasma ionisation multi-collector mass spectrometer (PIMMS): the ThermoFinnigan Neptune. Plasma Source Mass Spectrometry. Spec. Pub. Royal Society of Chemistry, 307-320.

Pearson, DG, Nowell, GM, 2005. Accuracy and precision in plasma ionisation multi-collector mass spectrometry: Constraints from neodymium and hafnium isotope measurements. Plasma Source Mass Spectrometry, Current Trends and Future Developments, 284-314.

Potts, PJ, Tindle, AG, Webb, PC, 1992. Geochemical reference material compositions: rocks, minerals, sediments, soils, carbonates, refractories and ores used in research and industry. Whittles Publishing, Caithness, U.K.

Royse, K, Kempton, PD, Darbyshire, DPF, 1998. NERC Isotope Geosciences Laboratory Report Series, 121.

Sitorus, K, 1990. Volcanic stratigraphy and geochemistry of the Idjen Caldera Complex, East Java, Indonesia. MSc thesis, University of Wellington, New Zealand.